NAVAL POSTGRADUATE SCHOOL

MONTEREY, CALIFORNIA

THESIS

INTRASEASONAL, LARGE-SCALE CIRCULATIONS AND TROPICAL CYLCONE ACTIVITY OVER THE WESTERN NORTH PACIFIC DURING BOREAL SUMMER

by

Tracey Lee Delk

June 2004

Thesis Advisor:	Patrick Harr
Second Reader:	Russell Elsberry

Approved for public release; distribution is unlimited.

THIS PAGE INTENTIONALLY LEFT BLANK

REPORT DOCUMENTATION PAGE			Form Approved OHPA No. 0704-0188
Public reporting burden for this collection of information is estimated to average 1 hour per response, including the time for reviewing instruction, searching existing data sources, gathering and maintaining the data needed, and completing and reviewing the collection of information. Send comments regarding this burden estimate or any other aspect of this collection of information, including suggestions for reducing this burden, to Washington headquarters Services, Directorate for Information Operations and Reports, 1215 Jefferson Davis Highway, Suite 1204, Arlington, VA 22202-4302, and to the Office of Management and Budget, Paperwork Reduction Project (0704-0188) Washington DC 20503.			
1. AGENCY USE ONLY ***(Leave blank)***	**2. REPORT DATE** June 2004	**3. REPORT TYPE AND DATES COVERED** Master's Thesis	
4. TITLE AND SUBTITLE: Intraseasonal, Large-scale Circulations and Tropical Cyclone Activity over the Western North Pacific during Boreal Summer		**5. FUNDING NUMBERS**	
6. AUTHOR(S) Tracey Lee Delk			
7. PERFORMING ORGANIZATION NAME(S) AND ADDRESS(ES) Naval Postgraduate School Monterey, CA 93943-5000		**8. PERFORMING ORGANIZATION REPORT NUMBER**	
9. SPONSORING /MONITORING AGENCY NAME(S) AND ADDRESS(ES) Office of Naval Research Arlington, VA 22217		**10. SPONSORING/MONITORING AGENCY REPORT NUMBER**	
11. SUPPLEMENTARY NOTES The views expressed in this thesis are those of the author and do not reflect the official policy or position of the Department of Defense or the U.S. Government.			
12a. DISTRIBUTION / AVAILABILITY STATEMENT Approved for public release; distribution is unlimited.		**12b. DISTRIBUTION CODE**	

13. ABSTRACT (maximum 200 words)

Large-scale circulations in the 15-25 day period over the western North Pacific during northern summer were determined using the leading modes of a Singular Value Decomposition of 850 hPa winds and outgoing longwave radiation. Composites were constructed to define the wave patterns' structural characteristics. Their evolution is characterized by alternating cyclonic and anticyclonic equatorial anomalies that are linked to anomalous convective activity. Mid-latitude perturbations appear to contribute to the growth of new equatorial disturbances.

Variability within the cycle is examined relative to variations in the basic state vertical wind shear and zonal wind convergence or divergence in the region equator-10ºN, 140ºE-160ºE. For the 50 cases in a basic state with easterly vertical wind shear and convergence, westward-moving waves propagate farther northwestward, wavelength contraction is greater, their orientation changes from east-west to southwest-northeast, and waves appear to be coupled with a Southern Hemisphere mid-latitude wave train. For the zonal wind divergence set, wave activity occurs farther eastward, circulations maintain a longer wavelength and more zonal orientation, and linkage with the Southern Hemisphere mid-latitudes is minimal.

A statistically-significant relationship exists between the 15-25 day wave phase and tropical cyclone activity. Formation frequency and preferred locations are modulated by the 15-25 day wave.

14. SUBJECT TERMS Tropical Cyclones, Equatorial Rossby Waves, Large-scale Tropical Circulations			**15. NUMBER OF PAGES** 95
			16. PRICE CODE
17. SECURITY CLASSIFICATION OF REPORT Unclassified	**18. SECURITY CLASSIFICATION OF THIS PAGE** Unclassified	**19. SECURITY CLASSIFICATION OF ABSTRACT** Unclassified	**20. LIMITATION OF ABSTRACT** UL

NSN 7540-01-280-5500

Standard Form 298 (Rev. 2-89)
Prescribed by ANSI Std. 239-18

THIS PAGE INTENTIONALLY LEFT BLANK

Approved for public release; distribution is unlimited.

INTRASEASONAL, LARGE-SCALE CIRCULATIONS AND TROPICAL CYCLONE ACTIVITY OVER THE WESTERN NORTH PACIFIC DURING BOREAL SUMMER

Tracey L. Delk
Lieutenant, United States Navy
B.S., United States Naval Academy, 1996

Submitted in partial fulfillment of the
requirements for the degree of

**MASTER OF SCIENCE IN
METEOROLOGY AND PHYSICAL OCEANOGRAPHY**

from the

**NAVAL POSTGRADUATE SCHOOL
June 2004**

Author: Tracey Lee Delk

Approved by: Patrick Harr
Thesis Advisor

Russell Elsberry
Second Reader

Chuck Wash
Chairman, Department of Meteorology

THIS PAGE INTENTIONALLY LEFT BLANK

ABSTRACT

Large-scale circulations in the 15-25 day period over the western North Pacific during northern summer were determined using the leading modes of a Singular Value Decomposition of 850 hPa winds and outgoing longwave radiation. Composites were constructed to define the wave patterns' structural characteristics. Their evolution is characterized by alternating cyclonic and anticyclonic equatorial anomalies that are linked to anomalous convective activity. Mid-latitude perturbations appear to contribute to the growth of new equatorial disturbances.

Variability within the cycle is examined relative to variations in the basic state vertical wind shear and zonal wind convergence or divergence in the region equator-10ºN, 140ºE-160ºE. For the 50 cases in a basic state with easterly vertical wind shear and convergence, westward-moving waves propagate farther northwestward, wavelength contraction is greater, their orientation changes from east-west to southwest-northeast, and waves appear to be coupled with a Southern Hemisphere mid-latitude wave train. For the zonal wind divergence set, wave activity occurs farther eastward, circulations maintain a longer wavelength and more zonal orientation, and linkage with the Southern Hemisphere mid-latitudes is minimal.

A statistically-significant relationship exists between the 15-25 day wave phase and tropical cyclone activity. Formation frequency and preferred locations are modulated by the 15-25 day wave.

THIS PAGE INTENTIONALLY LEFT BLANK

TABLE OF CONTENTS

THIS PAGE INTENTIONALLY LEFT BLANK

LIST OF FIGURES

LIST OF TABLES

THIS PAGE INTENTIONALLY LEFT BLANK

ACKNOWLEDGMENTS

I would like to extend my thanks to Professor Patrick Harr for his patience, flexibility, and guidance throughout the thesis process. Pat, please accept my best wishes for your future success.

To Andrew, the sparkle in my life, thank you for your understanding and encouragement.

Finally, to my parents, thank you for your continuing love and support. Everything that I have accomplished in my life is a direct result of your dedication and belief in me. I have been truly blessed.

THIS PAGE INTENTIONALLY LEFT BLANK

I. INTRODUCTION

A. OBJECTIVE

The United States Navy has long been interested in tropical cyclone prediction for safety of ships and aircraft, both in harbor and at sea, and for disaster preparedness of shore establishments. The Chief of Naval Operations' vision, "Sea Power 21: Projecting Decisive Joint Capabilities," which describes the future of U.S. naval operations, increases the importance of improved long-range tropical cyclone forecast prediction. Three basic concepts form the foundation of Sea Power 21: Sea Strike, Sea Shield, and Sea Basing. The primary focus of these three ideas is to control the seas and use the sea-based theater as a large maneuver area, and thus limit the U.S. military's dependence on land bases. Sea Basing is the concept that allows Sea Strike and Sea Shield to become realities. Sea Basing will allow commanders afloat the command and control and logistics support through a network of sea-based platforms (Clark 2002). Long-range tropical cyclone forecasts will enhance the execution of Sea Power 21 by providing planners with the tools to make decisions as to where the sea-based platforms should be placed to be used most effectively in an operation.

Long-range tropical cyclone prediction is a complex problem due to the lack of observational data, the variety of scales of motion present in the tropics, and an incomplete understanding of the dynamics associated with tropical cyclone formation. The objective of this study is to examine the large-scale circulations that force sub-monthly periods of enhanced and reduced convection over the western North Pacific during the Northern Hemisphere summer to establish the impact of these anomalous convection periods on tropical cyclone activity.

B. MOTIVATION

Large-scale winds over the tropical western Pacific exhibit significant synoptic-scale variability over interannual, seasonal, intraseasonal, and synoptic

periods. The El Niño- Southern Oscillation (ENSO) has a multi-year frequency and varies in strength, intensity, and period. ENSO is characterized by an increase in westerlies in the equatorial tropics (Rasmussen and Carpenter 1982). Takayuba and Nitta (1993) determined that convective disturbances that occur in the three- to five- day period are affected during both El Niño and La Niña. La Niña, which occurs on the same frequency as ENSO, is characterized by an increase in the easterlies in the tropics (Rasmussen and Carpenter 1982). The Madden-Julian Oscillation (MJO) varies with a period from twenty to eighty days (Madden and Julian 1994). The MJO eastward-propagating convective envelope is accompanied by upper-level wind anomalies, such that these anomalies are easterly west of the envelope and westerly east of the envelope. At smaller time scales, circulation and convection patterns are connected to convectively-coupled, equatorially-trapped waves such as Kelvin waves, equatorial Rossby waves, and mixed Rossby-gravity (MRG) waves. Typically, Kelvin waves occur on the three- to twenty- day period, while equatorial Rossby waves occur in the ten- to fifteen- day period and MRG waves occur in the three- to six- day period (Wheeler and Kiladis 1999). However, considerable variability exists with periods of these wave types. Over the western North Pacific, all of the above circulation systems over the tropical oceans have some relation to the large-scale fluctuations in the monsoon trough (Harr and Elsberry 1991, 1995), which may then impact tropical cyclone activity. If specific relationships exist between those circulation systems that vary on interannual and intraseasonal scales and the tropical cyclone formations, then the slowly varying features may be used in extended range prediction schemes for tropical cyclone activity.

C. BACKGROUND

Matsuno (1966) developed the theoretical treatment for equatorially-trapped tropical waves in which both Kelvin and Rossby waves could be trapped along the equator. Kelvin waves propagate eastward at the speed of a gravity wave with particle velocities that are predominately parallel to the equator. Rossby waves propagate westward with meridional wave motions that may induce a strong zonal velocity along the equator. Whereas the Rossby wave is in

approximate geostrophic balance, the MRG wave has mixed characteristics of gravity and Rossby waves. The pressure gradient and wind velocity fields are nearly geostrophic at high latitudes and winds are ageostrophic near the equator. This Matsuno theoretical treatment is the basis of all tropical wave studies and will be the foundation for this study.

Since Matsuno, observational and theoretical tropical meteorologists have further developed the ideas of tropical waves to include wave initiation and development, vertical and horizontal wave structures, and especially the convective variability associated with each wave type. Furthermore, considerable research has been done to identify relationships between equatorial wave activity and other large-scale tropical circulation systems. In particular, many studies have linked the synoptic-scale waves to circulations that vary over long time scales and large space scales (e.g., ENSO and MJO). These relationships are summarized below for the western North Pacific region in relation to potential impacts on tropical cyclone activity.

1. El Niño and La Niña

Chan (1999) identified the role of El Niño and La Niña in tropical cyclone activity. He found that tropical cyclone activity is below normal in the South China Sea and above normal in the western North Pacific during September and October of an El Niño year. During a La Niña year, the opposite is true. These anomalies in activity appear to be linked to large-scale flow anomalies at 850 hPa and 500 hPa. Takayuba and Nitta (1993) discussed westward-propagating disturbances (MRG and tropical depression (TD-type)) and their structural changes due to the changes in the large-scale environment related to ENSO. The MRG waves generally occur east of 160º E and may evolve to TD type waves near 150ºE. During El Niño, when 850 hPa westerly winds extend toward the dateline, the MRG wave activity shifts toward the eastern Pacific and TD type disturbances dominate the central Pacific. Thus, the transition zone shifts eastward with the eastward shift in westerly winds. During La Niña, 850 hPa easterly winds extend westward through the Philippine Sea. Thus, the MRG

disturbances extend into the western Pacific and the transition to TD-type waves occurs farther to the west. These transition zone shifts indicate that individual disturbances are influenced by changes in the local environment due to the larger scale, slowly varying ENSO influence. Whereas environments with small horizontal and vertical wind shear and easterly background flow will preferentially support MRG type disturbances, environments with easterly vertical shear and westerly background flow (typical of monsoon regions) will tend to favor more TD-type disturbances.

2. Madden-Julian Oscillation

The role of the MJO in development or modification of equatorial disturbances has been studied and found to be a precursor of western Pacific tropical cyclones (Liebmann et al. 1994). Rossby waves develop west of the MJO forcing, and Kelvin waves develop to the east. Dickinson and Molinari (2002) found a sequence of TD-type waves led to tropical cyclone formations as an active phase of the MJO propagated eastward through the western North Pacific. Aiyyer and Molinari (2003) conducted a modeling study using a shallow water system that idealized the MJO as a mass sink. They discovered that energy is transferred from larger to smaller scales in the areas of large-scale basic state convergence due to the MJO. At least during the active phase, the large-scale, slowly-varying MJO contributes to the growth of smaller-scale disturbances.

3. Monsoon Trough

Monsoon regions are typified by high outgoing long-wave radiation (OLR) variance, high kinetic energy, and equatorial westerly winds (Liebmann and Hendon 1990). Monsoon trough variability affects tropical cyclone formation and track characteristics. Harr and Elsberry (1991, 1995) note that active periods of the monsoon trough that are associated with enhanced large-scale convection are characterized by anomalous convergence at 700 hPa and divergence at 200 hPa. Therefore, an active monsoon trough defines a basic state that would be conducive to the growth of smaller-scale wave disturbances. Additionally, anomalous large-scale cyclonic shear created by increased equatorial westerlies

due to cross-equatorial flow from the Southern Hemisphere acts to alter the tracks of western North Pacific tropical cyclones that form south of 20ºN and west of 150ºE or south of 10ºN and east of 150ºE.

4. Equatorially-Trapped Waves

a. Kelvin Waves

Kelvin waves in the equatorial region propagate eastward along the equator with speeds of 15 – 20 m s^{-1} over periods of three to twenty days and are symmetric with respect to the equator (Gill 1982; Wheeler and Kiladis 1999). Convectively-coupled Kelvin waves are generally a response to an upper-tropospheric heat source during boreal summer that may be forced by anomalous divergence due to equatorward-propagating waves from the Southern Hemisphere (Straub and Kiladis 2003b). During this season, the subtropical jet (STJ) in the Southern Hemisphere is in its northernmost position and at its maximum amplitude. Therefore, those wave sources can be in the form of lower-tropospheric pressure surges in the winter hemisphere or as an upper-tropospheric trough propagating equatorward through the tropics during winter.

b. Equatorial Rossby Waves

Equatorial Rossby waves propagate westward at five to ten meters per second over a period of ten to 15 days. Typically, variance in convection associated with Rossby waves is much greater than that for Kelvin waves and has similar amplitude variability to that of the MJO (Wheeler and Kiladis 1999). This convective variability suggests that Rossby wave activity may also be sensitive to alterations in the large-scale circulations. Excitation of these waves is thought to occur by two mechanisms: deep convection and upper-level activity from the extratropics. Kiladis (1998) suggests that upper-level wave activity propagates into the tropics at 200 hPa from the winter hemisphere along great circle routes using the tropopause as a wave guide. This propagation of vorticity into the tropics then acts to generate equatorial Rossby waves. At 850 hPa, cyclonic anomalies appear west of the upper-level cyclones and modulate the convection within the monsoon trough. Kiladis noted that paired cyclonic disturbances propagate along the equator at low levels, west of monsoon trough

convection. Alternately, when easterlies vice westerlies occur throughout a deep layer in the tropics, these upper-level Rossby waves cannot propagate into the tropics and excite equatorial Rossby waves.

c. Coupled Kelvin-Rossby Waves

Gill (1980) discussed solutions for tropical circulations induced by diabatic heating. His simple model for circulations based on symmetric forcing about the equator indicates an east-west asymmetry relative to the area of heating. East of the region of heating, low-level easterlies propagate eastward through the generation of Kelvin waves. West of the region of heating, Rossby waves develop and contribute to low-level westerlies. Thus, areas of heating that are often indicated by regions of deep convection can generate coupled Kelvin-Rossby waves.

d. Mixed Rossby-Gravity Waves and Tropical Depression Type Disturbances

Mixed Rossby-gravity (MRG) waves are convectively coupled and are second only in frequency of occurrence to Rossby waves (Wheeler and Kiladis 1999). MRG waves are often found in the central Pacific and propagate westward at 15-20 m s^{-1} with periods of three to six days and wavelengths of 7,000 to 10,000 km. However, MRG waves in the western Pacific tend to have slower phase speeds and shorter wavelengths (Liebmann and Hendon 1990). For example, Aiyyer and Molinari (2003) state that central Pacific MRG waves have phase speeds of 15 to 20 m s^{-1} and wavelengths of 6000 to 10,000 km while western Pacific MRG waves have phase speeds of 3.5 to 4 m s^{-1} and wavelengths of 3000 km.

Takayuba and Nitta (1993) differentiate between tropical depression (TD-type) disturbances and MRG disturbances based on horizontal structure and phase relationships to convective activity. TD-type disturbances, sometimes known as easterly waves, are off-equatorial vortices with convection organized about a low-pressure cyclonic circulation. Generation mechanisms and locations of TD-type disturbances are controversial and the several different theories have been proposed. Although generation mechanisms are uncertain,

the current viewpoint is that maintenance of these disturbances is through diabatic effects from convective processes. In observed MRG-type disturbances, which have structures similar to linear MRG waves, convection is associated with the low-level convergence regions in the wave. Takayuba and Nitta (1993) also determined that when a disturbance is within the easterly trades where the mean flow is about 5 m s^{-1} westward, and only small horizontal shear exists, the structure will tend to take on the form of an MRG-wave-type disturbance. Conversely, if a disturbance is under the influence of a monsoon trough in a region of light winds and large cyclonic shear, it will take on the structure of a TD-type disturbance. Additionally, other environments may support each type of disturbance and not all MRG-wave-type disturbances develop into TD-type disturbances.

5. Synopsis

The above summary highlights that the occurrence and structure of the primary tropical synoptic-scale disturbances over the western North Pacific vary based on several factors associated with the large-scale basic state over the region. Furthermore, the basic state may be influenced by several slowly-varying, global-scale circulation systems.

Whereas many of the circulation systems identified have been shown to influence tropical cyclone activity over varying time scales, this thesis concentrates on tropical circulations with 15 – 25 day periods that have been identified to contain a significant amount of variance over the western North Pacific. Characteristic circulation modes of 15 – 25 day circulations will be identified. Periods of enhanced 15 – 25 day variability will be examined to determine the source of variability and relationships to other tropical circulation modes defined above. The concluding section will examine the likely control of tropical cyclone activity by these 15 – 25 day modes.

THIS PAGE INTENTIONALLY LEFT BLANK

II. METHODOLOGY

A. DATA

The data used for this study are 2.5º latitude by 2.5º longitude global gridded reanalysis fields from the National Centers for Environmental Prediction (Kalnay et al., 1996) for the years 1979 to 2000. Outgoing long-wave radiation (OLR) data on 2.5 º latitude by 2.5º longitude grid (Liebmann and Smith 1996) are used as a proxy for deep convection. The OLR data are global in longitude between 30ºS and 30ºN. The data were averaged daily for every year to determine a daily climatological mean. Once the mean was calculated, daily anomalies for each field were calculated by subtracting the daily mean and then the fields were filtered with a Lanczos filter (Duchon 1979) to isolate the 15- to 25-day disturbances.

B. SINGULAR VALUE DECOMPOSITION

The technique of singular value decomposition [Bretherton et al., 1992, (SVD)] of OLR and 850 hPa winds is used to identify the coupled modes of 15- to 25-day variability that define a modulation of equatorial convection between 150ºE and 170º E. The leading SVD modes identify several wave-like patterns that are related to covariability in equatorial convection and tropical, subtropical, and mid-latitude anomalous circulations. Furthermore, covariability between OLR and circulations in the Southern and Northern Hemisphere mid-latitudes is identified. Time coefficients associated with the leading modes identify periods of enhanced and reduced 15- to 25-day variability.

C. COMPOSITES

Composites for anomalies of heights, winds, relative humidity, vertical motion (omega), and temperatures were developed based on SVD time coefficients for each year. When SVD mode 2 leads SVD mode 1 by 90º, it represents an active 15 to 25 day phase. Each active phase is divided into eight groups of 45º. The fields of variables for each group are combined to create eight composites for each field (Fig. 1). The objective is to identify the

relationship between the wave patterns and regions of OLR variability and what environmental factors control the relationship.

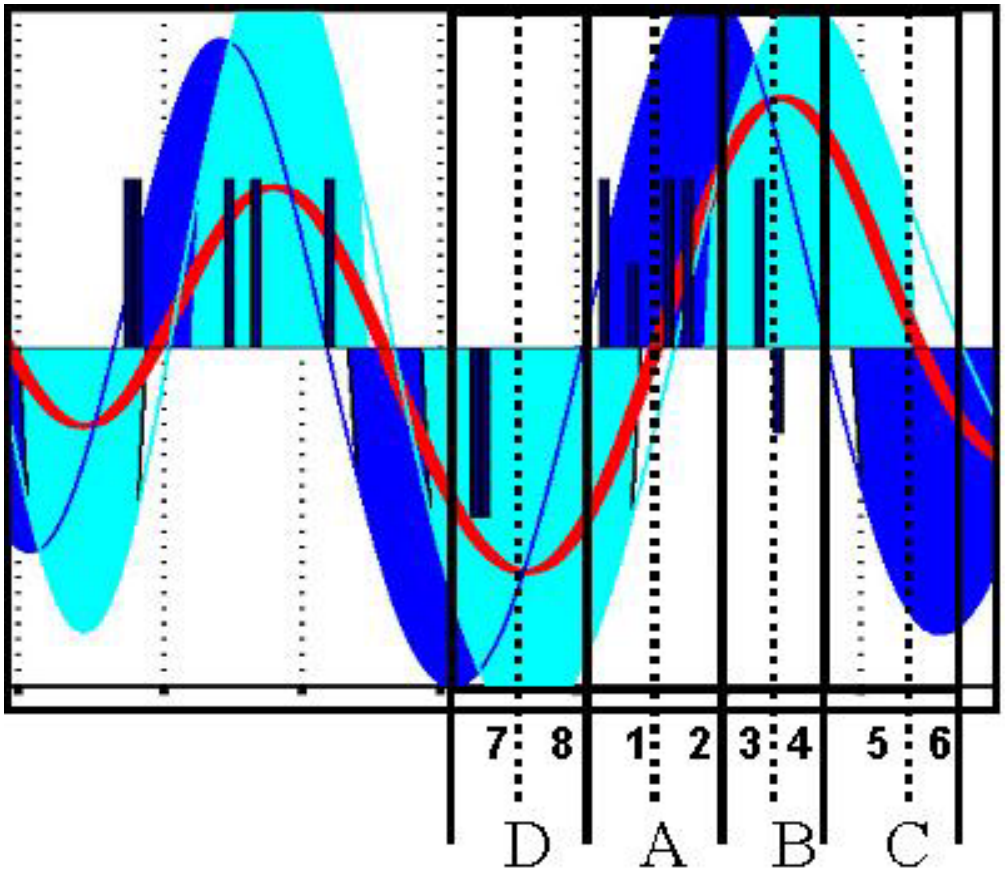

Figure 1. Example time series of two SVD coefficients (dark blue and light blue lines) that are approximately in quadrature. Four phases (labeled A- D) are defined based on 90º phase divisions and eight phases (labeled 1- 8) are defined based on 45º phase divisions. Typical 850 hPa wind anomalies over the monsoon trough region of the western North Pacific are defined by the red line.

III. ANALYSIS

Some periods of enhanced or reduced tropical cyclone activity may coincide with slowly-varying large-scale events such as the MJO and others may not. Because of the important relationship between low-level zonal wind and tropical cyclone activity (Harr and Elsberry 1995), the relationships of the variability of low-level zonal wind to large-scale circulation modes are important. Furthermore, the dependence of OLR, low-level convergence, and vertical wind shear on large-scale circulation modes is of interest. Finally, the potential coupling of Southern Hemisphere circulations with Northern Hemisphere circulations that are associated with tropical cyclone activity may define an important forcing mechanism for the large-scale and slowly-varying circulation modes with 15-25 day periods.

A. SVD PATTERNS

1. Background

The singular value decomposition (SVD) patterns were developed by constructing a combined cross-covariance matrix using wind components (u, v) and OLR. The matrix is combined in the sense that u and v are both included as an augmented matrix in the computation of the cross-covariance with OLR. An SVD of the cross-covariance matrix results in the definition of a spatially orthogonal set of patterns (i.e. modes). Additionally, a synthetic time series is formed for each mode as a linear combination of the patterns.

Following Bretherton et al. (1992), there are N_w cases of wind observations and N_o cases of OLR observations. The wind observations are contained in a matrix $\overline{W}(t)$ while the OLR observations are contained in $\overline{O}(t)$. The $N_w \times N_o$ cross-covariance matrix is defined as

$$\overline{C}_{wo} \equiv \left\langle \overline{W}(t)\overline{O}(t) \right\rangle$$

where $\langle\ \rangle$ defines a time average. The matrix $\overline{C}_{wo}$ is decomposed as

$$C = \sum_{k=1}^{M} \sigma_k L_k R_k^T , \qquad \text{where } \left[M \le \min\left(N_w, N_o\right) \right].$$

The orthogonal set of M vectors contained in L_k defines the left singular vectors, which in this case are identified with the wind fields. The orthogonal set of M vectors in R_k defines the right singular vectors, which correspond to the OLR fields. The non-negative σ_k are the singular values, which are ordered from the largest to smallest. Finally, the expansion coefficients, which define the linear relationships between each observation (e.g., wind and OLR fields) and each singular vector, are defined as $a_k(t) = L_k \bullet \overline{W}_k(t)$ for the wind fields and $b_k(t) = R_k \bullet \overline{O_k}(t)$ for the OLR fields.

Results are displayed as heterogeneous correlation maps. The k^{th} heterogeneous correlation map for the wind fields is defined as the vector of correlation coefficients between gridpoint values of the wind fields and the k^{th} expansion coefficient of the OLR field. The interpretation of the heterogeneous correlation map for the wind fields is that it defines how well the gridpoint values of the wind fields could be predicted from the k^{th} OLR expansion coefficient. Similarly, heterogeneous correlation maps for the OLR fields can be computed by interchanging fields and expansion coefficients.

2. Results

Heterogeneous correlation maps (Figs. 2, 3) are plotted with wind correlations depicted as streamlines such that the horizontal and meridional components are defined by the u-correlation and v-correlation values, respectively. The OLR correlation values are shaded. Only statistically significant values are plotted.

a. Mode 1

A cyclonic circulation over the Philippines is tilted southwest to northeast (Fig. 2). Strong southwesterly winds are associated with enhanced convection over the Philippine Sea that extends southwestward over the South

China Sea. An anticyclonic anomaly is southeast of the cyclonic circulation with an area of reduced convection at the equator that extends into the Southern Hemisphere. Additionally, a hint of a wave train extends from the region of enhanced convection into the Northern Hemisphere mid-latitudes. As part of the wave train, northerly anomalies extend toward the equator over the eastern North Pacific between 170°W-150°W.

b. Mode 2

A cyclonic anomaly is over the Philippine Sea. Southwesterly anomalies are associated with enhanced convection that is centered in the southerly anomalies between the cyclonic anomaly and an anticyclonic anomaly to the east. There is an indication of a wave train in the Southern Hemisphere that extends toward the equator east of Australia. The equatorward extension of this wave train comprises one cell of a quadripole circulation pattern that is similar to an equatorial Rossby-wave type pattern. Other circulations in this quadripole pattern include a Southern Hemisphere anticyclone that is along 160°W and the Northern Hemisphere cyclonic and anticyclonic circulations described above. A Northern Hemisphere mid-latitude wave train is also evident in this mode.

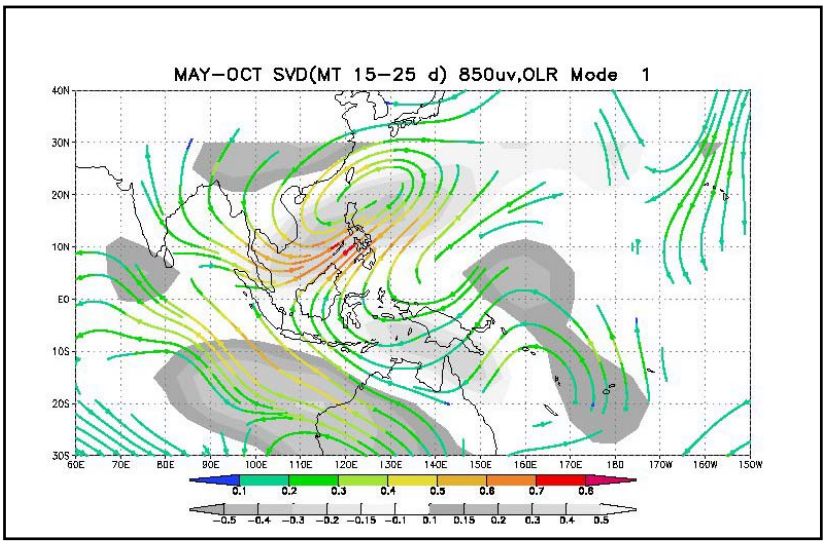

Figure 2. Mode 1 heterogeneous correlation map for 850 hPa u- and v- correlation coefficients (streamlines, no units) and OLR-correlation coefficients (shaded, no units) . Only significant values are plotted.

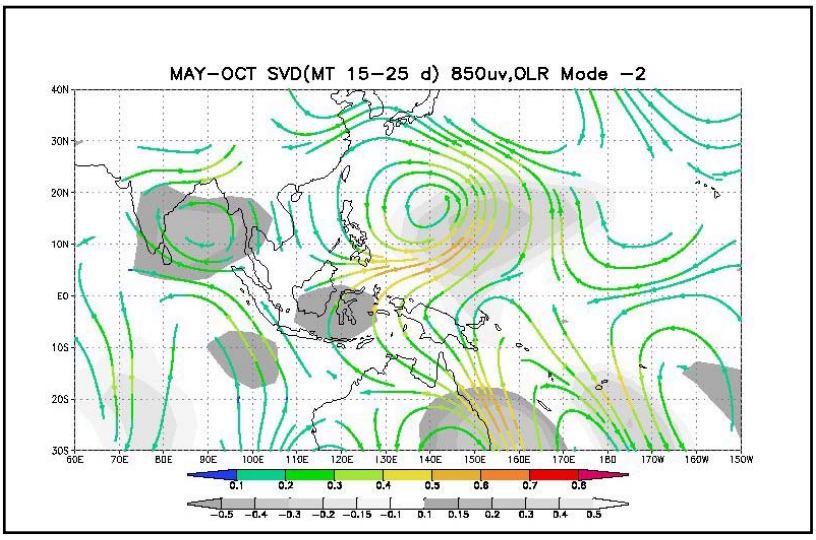

Figure 3. Same as in Figure 2, except for mode 2.

c. SVD Coefficients [May – Oct 1979-2000]

A comparison of the time coefficients (Figs. 4, 5, 6) for modes 1 (light curve) and 2 (dark curve) suggests that mode 2 leads mode 1. The positive coefficients represent a pattern that is defined in Figures 2 and 3. The negative coefficients represent patterns of opposite sign. The vertical bars define tropical cyclone formation times with

- a long upward bar = formation in the monsoon trough region (equator to 20°N, 120°E to 150°E)
- a short upward bar = formation in the South China Sea (equator to 20°N, 100°E to 120°E)
- a short downward bar = formation east of the monsoon trough (equator to 20°N, 150°E to 180°)
- a long downward bar = formation north of the monsoon trough (20°N to 35°N , 110°E to 165°E).

Time periods that contain significant amplitudes for both coefficients and a phase relationship of mode 2 leading mode 1 by 90° define

periods of active 15 to 25 day modes (e.g., September 1980, September 15 to October 31, 1984). Note the amount of annual variability among the patterns. Several episodes occur in 1980, 1983, 1984, 1989, 1994, 1996, and 2000 while few episodes occur in 1982, 1988, 1992, 1995, and 1998. Perhaps the years with few episodes are related to ENSO as some of the years are post-El Niño years. The periods of active modes are used as the basis for the composites of anomalous physical quantities.

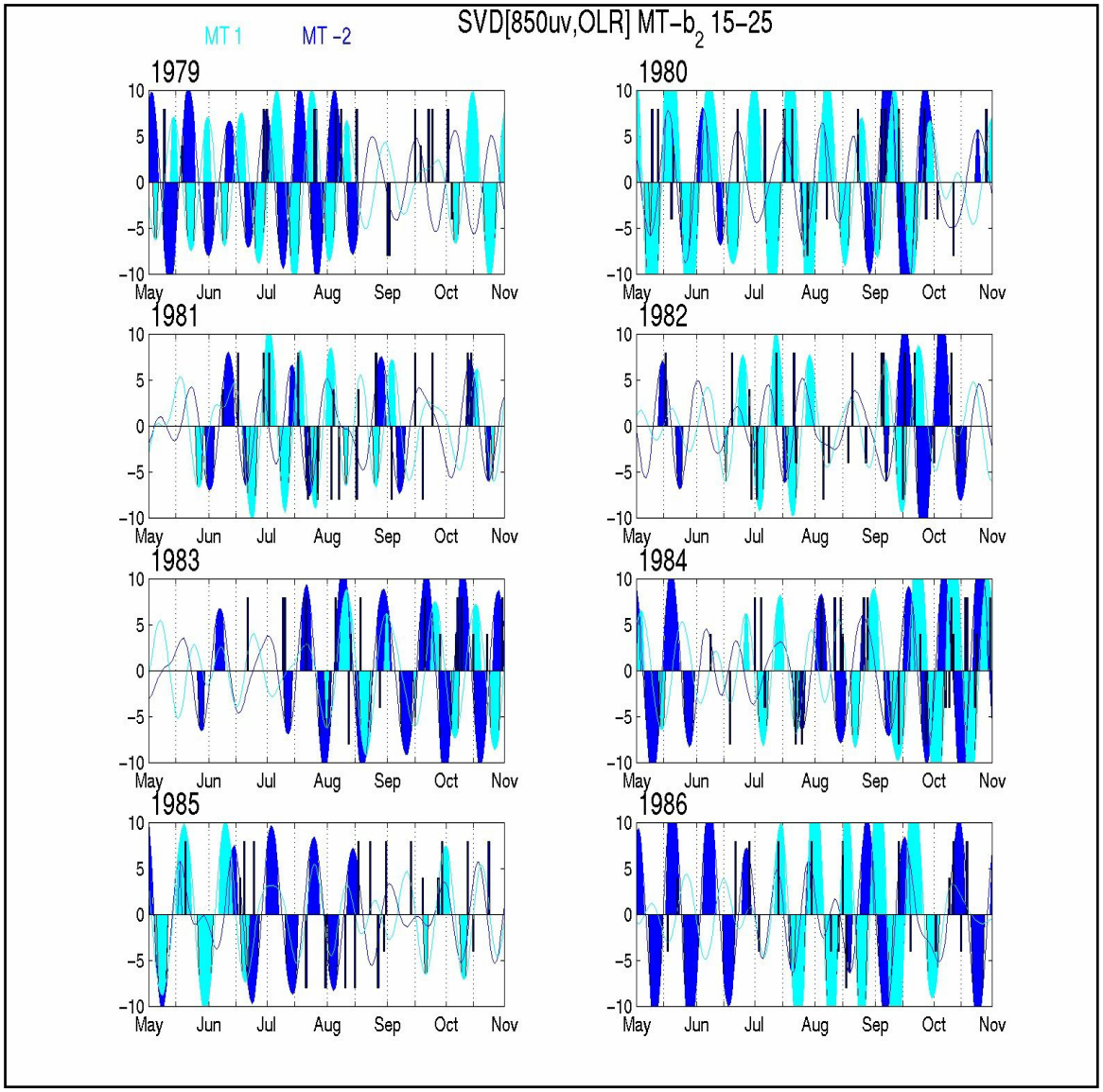

Figure 4. The leading two SVD coefficients of the 850 hPa winds and the OLR for 1979 – 1986. Curves are shaded when the amplitude of the mode is greater than the mean value plus or minus one standard deviation.

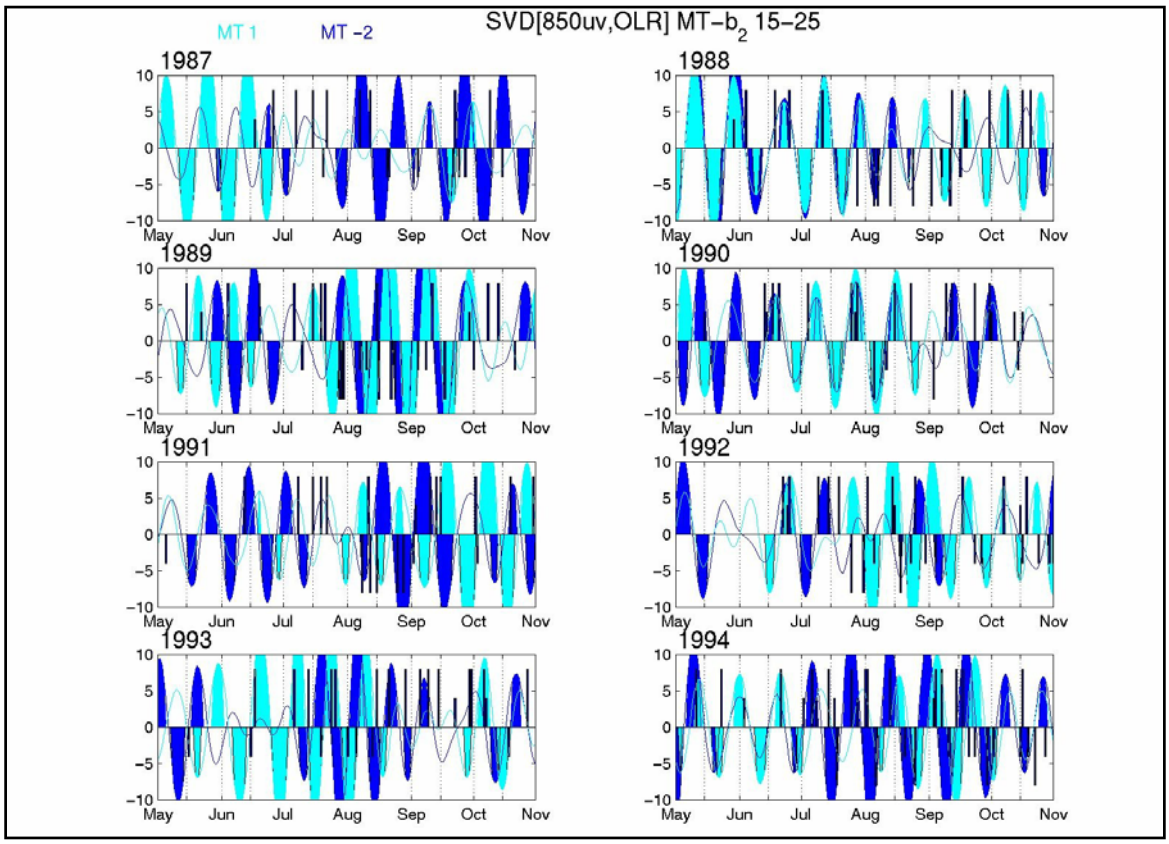

Figure 5. As in Fig. 4, except for 1987-1994.

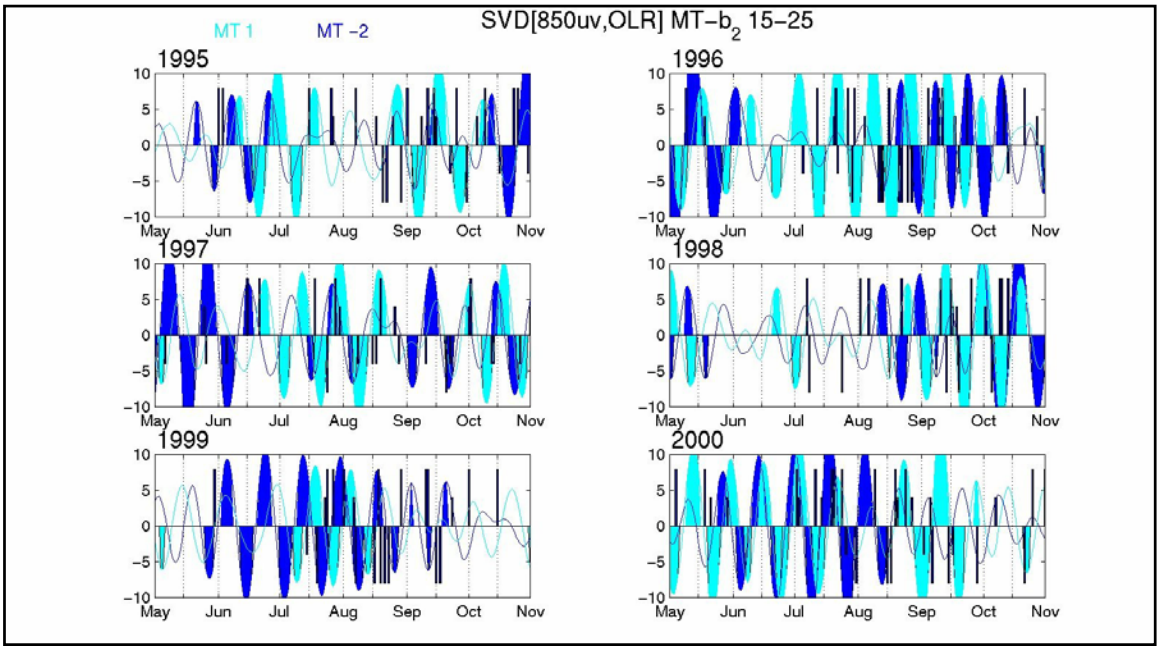

Figure 6. As in Fig. 5, except for 1995-2000.

B. COMPOSITES

Using the definitions of the eight phases (Fig. 1) based on the two SVD coefficients, composites of selected OLR fields for each phase will be presented and described. The objective is to describe the relationships between the variables as the atmosphere evolves through the eight phases of a 15 – 25 day cycle.

For the display of OLR and low-level circulation composites, only locally significant values of OLR are plotted. Local significance is determined by a t-test where the anomaly values are examined to determine if they are significantly different from zero. Likewise, for the wind fields, all streamfunction values are plotted but wind vectors are displayed only for anomalies that are significantly different from zero.

1. OLR and 850 hPa Winds

a. Phase 1

In Figure 7 (top), a large region of reduced convection (maximum OLR) has a southwest - northeast orientation that extends from the equator west of Indonesia to the mid-latitudes over the central North Pacific. A large area of anticyclonic wind anomalies (labeled as circulation 1) is associated with this region of reduced convection with the strong northeasterly wind anomalies near the area of largest OLR anomalies. A westward extension of circulation 1 (labeled 1a) is over Indochina. A mid-latitude anticyclonic anomaly (circulation 1b) is over the central North Pacific. A smaller region of reduced convection southwest of New Guinea is associated with an area of low-level diffluence along 10ºS.

In the Bering Sea, a cyclonic circulation with an associated trough extends into the central North Pacific. Across the central North Pacific between 30°N and 50°N, the combination of anticyclone, cyclone and weak anticyclone suggests a weak Rossby-wave response to the area of reduced convection over the tropical and subtropical western North Pacific.

A broad area of enhanced convection (minimum OLR) northwest of New Guinea extends southwest - northeast into the Northern Hemisphere and northwest - southeast into the Southern Hemisphere. The northern area is associated with a cyclonic wind anomaly, labeled 2, in the Northern Hemisphere. Two factors may be responsible for this cyclonic circulation. One may be Rossby-wave dispersion due to the anticyclone (circulation 1) to the northwest, which is associated with maximum OLR in the area of strongest northeasterly winds. A second factor is that the combination of the cyclonic anomaly centered near 7°N, 140°E with a cyclonic anomaly near 12°S, 165°E (labeled 3) represent an equatorial Rossby wave. The southern branch of enhanced convection is associated with the cyclonic anomaly (labeled 3) over the Coral Sea.

Additionally, an elongated northwest-southeast region of enhanced convection extends from the eastern Indian Ocean along 10ºS into Western Australia. This region is associated with strong poleward flow ahead of a large cyclonic anomaly.

b. Phase 2

In Figure 7 (bottom), the Northern Hemisphere and Southern Hemisphere regions of decreased convection in phase 1 have merged. This forms a horseshoe shape that extends to the northeast from the equator south of India into the mid-latitudes of the central North Pacific and to the southeast towards New Guinea and the northernmost tip of Australia. The extension of the area of reduced convection into the Bay of Bengal is associated with the westward movement of circulation 1a toward the Myanmar Peninsula. The maximum northeasterly anomalies over the South China Sea associated with circulation 1 have decreased in extent from phase 1 as circulation 1 has weakened. The trough over the central North Pacific present in phase 1 has become a closed cyclonic circulation (labeled 4) and has moved southeastward to 40°N, 170°W. The Rossby-wave response across the central North Pacific has become better defined in phase 2.

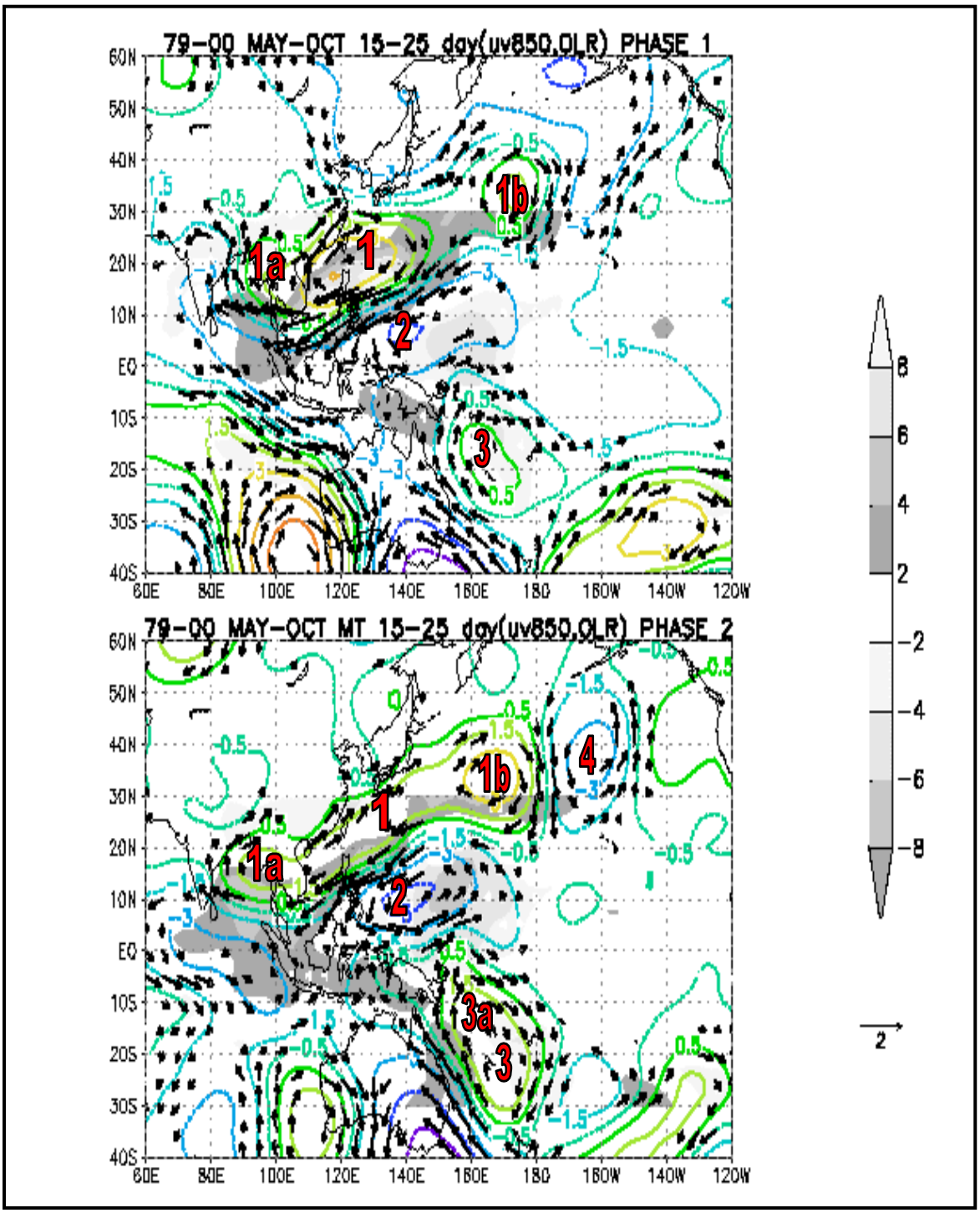

Figure 7. Phases 1 and 2 composites of 850 hPa significant winds (arrows) in m s^{-1} (scale at right), streamfunction (contour interval, 10^6 in m^2 s^{-1}), and OLR (shaded) in W m^{-2}.

Over the equatorial western Pacific, the region of enhanced convection associated with circulation 2 has increased in magnitude and now extends farther westward along 5ºN and also northwestward over the Philippine Sea. The westerlies just north of the equator associated with the strengthened cyclonic anomalies of circulation 2 have increased in magnitude. The cyclonic anomaly 3 in the Southern Hemisphere has moved southeastward toward New Caledonia and strengthened. The increased equatorward flow appears to converge with the westerlies along the equator and is associated with a region of enhanced convection and an extension of circulation 3 toward the equator (labeled 3a). Over the Southern Hemisphere, there is an indication of a mid-latitude wave train that begins with a weak anticyclone at 40°S, 80°E and extends across the southern portion of Australia. The strong cyclonic anomaly 3 and southerly flow east of Australia represent the most equatorward extension of the Southern Hemisphere wave train.

c. Phase 3

In Figure 8 (top), the region of reduced convection associated with circulation 1a has decreased in extent as circulation 1 has dissipated and only the anticyclone (1a) in the Bay of Bengal remains. These circulations support moderate easterlies along the equator that correspond with an area of reduced convection. The area of enhanced convection in the Philippine Sea has reached its maximum extent and intensity with the most negative OLR anomalies centered at 15ºN, 150ºE. In phase 3, the cyclonic anomaly (circulation 2) associated with the enhanced convection over the Philippine Sea has also intensified. The large cyclonic anomaly 3 in the Southern Hemisphere east of Australia has split such that the weaker anomaly 3a is centered at 5ºS, 140ºE and the larger circulation 3 has moved southeast to near the dateline as part of the Southern Hemisphere mid-latitude wave train. The winds associated with the weaker equatorial circulation 3a have merged with the westerlies of the northern cyclone 2 along 5ºN near 120ºE. Therefore, circulation 3a has remained coupled to circulation 2 while circulation 3 moves as a part of the Southern Hemisphere wave train.

Associated with the anomalous cyclonic circulation 2 over the Philippine Sea is a wave train that extends across the central North Pacific and includes circulations 1b and 4. In conjunction with this wave train, the anticyclonic circulation 1b near the dateline extends towards the equator. These anomalous winds define the start of an anticyclonic anomaly (labeled 5) near 15°N, 175°W. A similar development also occurs in the Southern Hemisphere where a weak anticyclonic anomaly (labeled 6) is found at 5°S, 175°W. Associated with this anticyclonic anomaly 6 is a developing area of reduced convection at 5°S, 170°E.

d. Phase 4

In Figure 8 (bottom), the region of decreased convection in the Indian Ocean has diminished in magnitude and area and has separated into a northern and a southern region. The northern area is associated with an anticyclonic anomaly 1a that has moved from the Bay of Bengal in phase 3 towards Sri Lanka in phase 4. The southern region of reduced convection is associated with southeasterly winds in the equatorward branch of a subtropical anticyclone that is west of Australia.

The area of enhanced convection over the western North Pacific associated with circulation 2 has propagated to the west and elongated along a southwest to northeast axis from Singapore in the southwest to 160ºE in the northeast. Over the mid-latitudes, the Rossby-wave train pattern has dissipated as circulation 1b has weakened. However, the near-equatorial anticyclonic anomaly (circulation 5) has become better defined to the southwest of Hawaii. The small region of decreased convection at 5°S, 170°E in phase 3 has increased in magnitude and area along 5°S between 160°E and the dateline. This area is associated with the anticyclonic anomaly 6 that may be coupled to the anticyclonic anomaly 5 in the Northern Hemisphere. Easterly anomalies are found along the equator between the anomalous anticyclones 5 and 6. Therefore, the combination of the two anticyclonic anomalies is indicative of an equatorial Rossby wave.

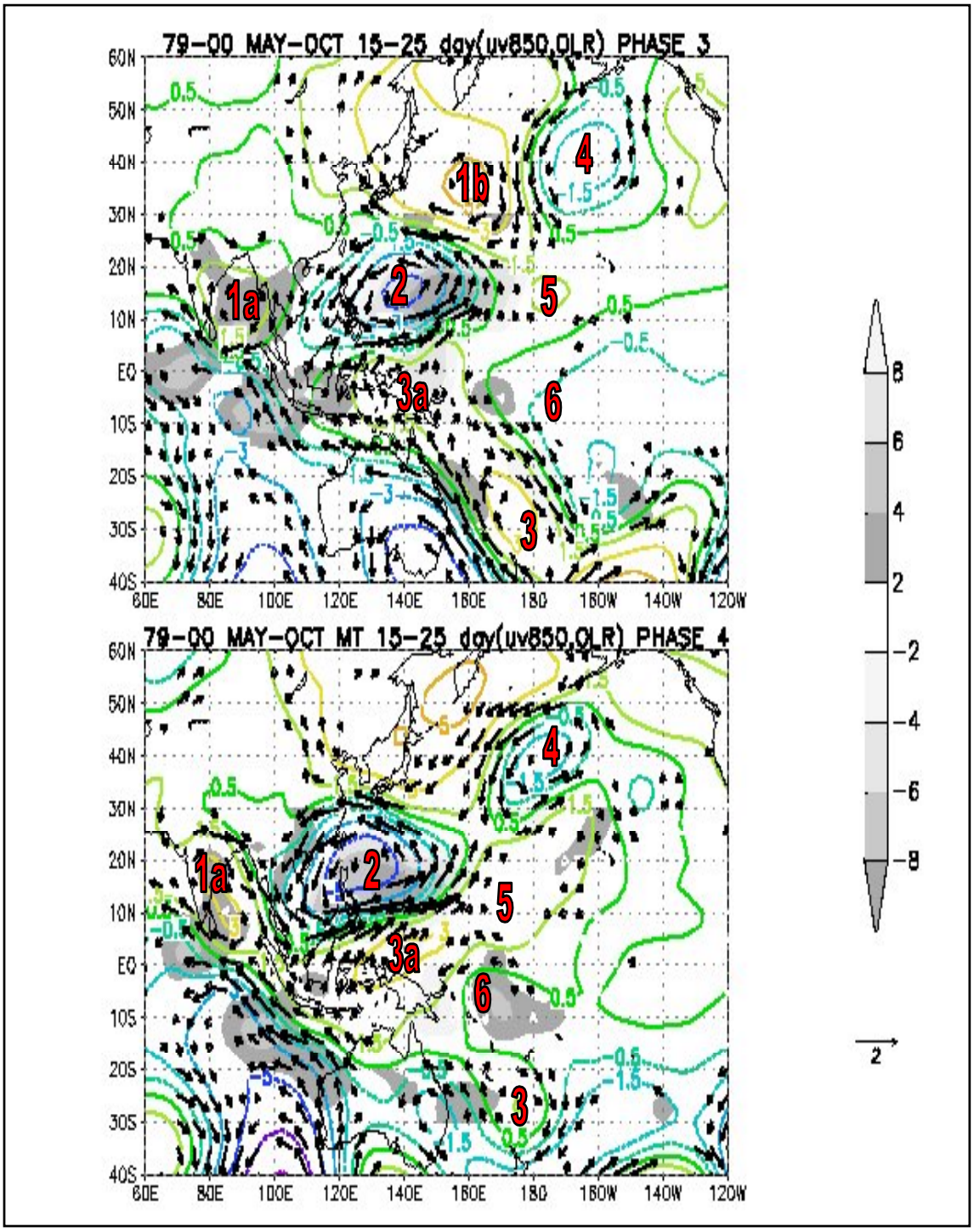

Figure 8. Phases 3 and 4 composites of 850 hPa significant winds (arrows) in m s^{-1} (scale at right), streamfunction (contour interval, 10^6 in m^2 s^{-1}), and OLR (shaded) in W m^{-2}.

e. Phase 5

In Figure 9 (top), the region of maximum enhanced convection associated with cyclonic anomaly 2 has decreased in areal coverage and has moved northwestward. Furthermore, the cyclonic anomaly 2 has weakened and elongated such that an extension (labeled 2a) exists over the Indochina Peninsula. The area of decreased convection in the Southern Hemisphere has expanded and extended northwestward into the Northern Hemisphere and southeastward into the Southern Hemisphere subtropics. This area of reduced convection is associated with the two anticyclonic anomalies 5 and 6 that straddle the equator between 140ºE and 170ºE. Strong easterlies along the equator associated with the northern and southern anticyclones correspond to the region of reduced convection. As discussed with respect to the development of the cyclonic anomaly 2 in phase 1, the intensification of the anticyclonic circulation 5 may be related to a combination of Rossby-wave dispersion from circulation 2 and the westward movement of circulation 5 from southwest of Hawaii in phases 3 and 4. The Southern Hemisphere anticyclone 6 that is centered near 15°S, 165°E appears to be developing as part of a wave train from the Southern Hemisphere mid-latitudes.

f. Phase 6

In Figure 9 (bottom), the region of enhanced convection associated with the cyclonic anomaly 2a has propagated westward along the equator near 70°E as the cyclonic anomaly 2a has moved westward. Associated with the movement of 2a towards the Bay of Bengal is a cyclonic circulation in the Southern Hemisphere at 5°S, 90°E (labeled 2c). The area of reduced convection associated with the anticyclonic anomalies 5 and 6 has increased in extent and propagated farther into the Northern Hemisphere. The associated anticyclonic circulation 5 has moved northwestward and intensified such that increased easterlies exist along the equator. The southern anticyclone 6 in the Coral Sea has elongated with an extension to the northwest (labeled 6a) that appears coupled to the northern anticyclone, 5. Over the Southern Hemisphere mid-latitudes, a wave train that encompasses the anticyclonic anomaly 6 has

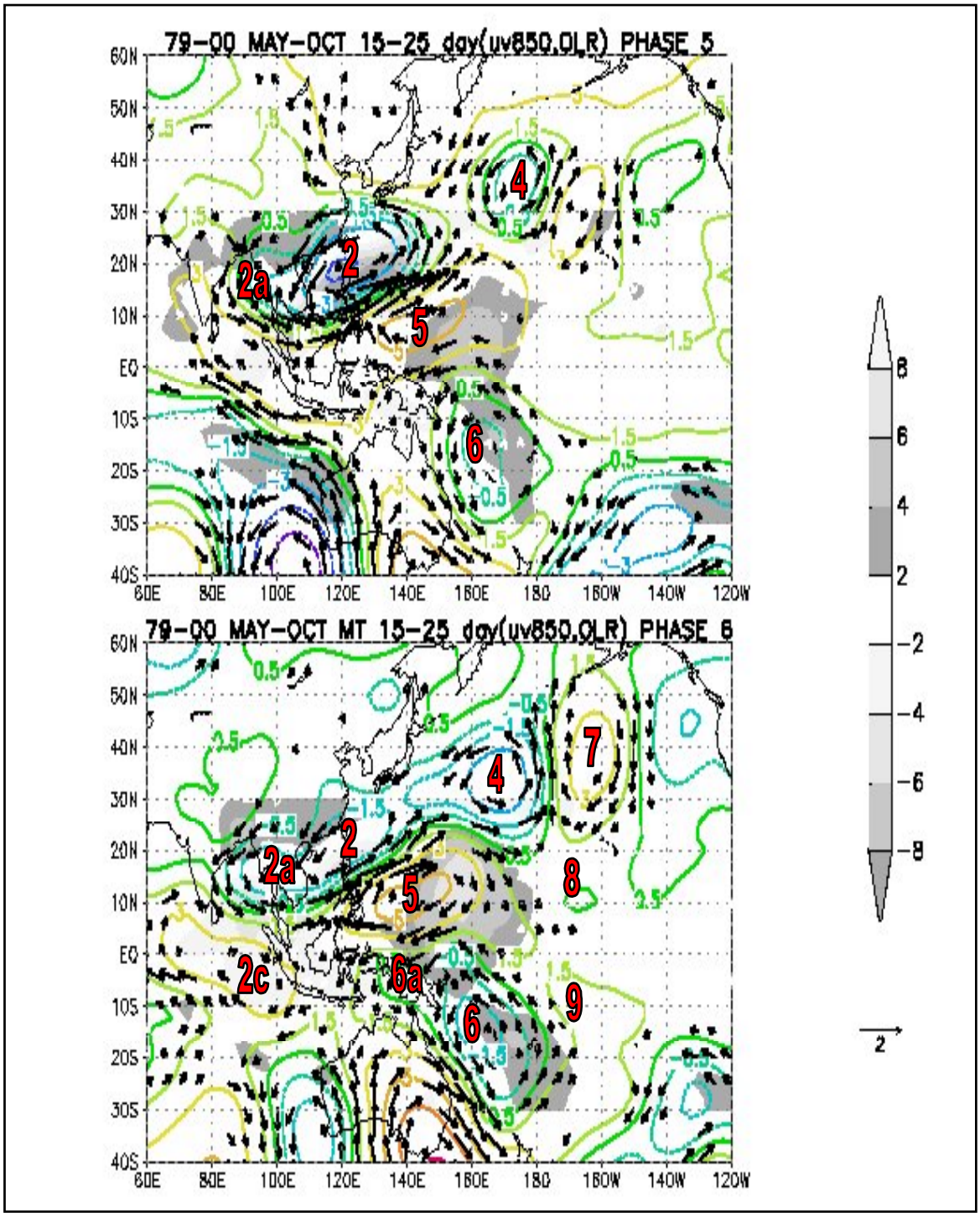

Figure 9. Phases 5 and 6 composites of 850 hPa significant winds (arrows) in m s^{-1} (scale at right), streamfunction (contour interval, 10^6 in m^2 s^{-1}), and OLR (shaded) in W m^{-2}.

amplified. In addition, a Northern Hemisphere wave response to the reduced convection and anticyclonic anomaly 5 has developed across the North Pacific. This wave train contains the cyclonic anomaly 4 and an anticyclonic anomaly 7. Associated with the cyclonic anomaly 4 is a trough that extends southwestward into the subtropics near 15°N, 170°W (labeled 8). A similar development has occurred in the Southern Hemisphere as a trough to the east of the anticyclonic anomaly 6 has contributed to a cyclonic anomaly near 10°S, 170°W (labeled 9).

g. Phase 7

In Figure 10 (top), the region of enhanced convection over the equatorial Indian Ocean has decreased and continued to propagate westward as the northern cyclonic anomaly 2a has weakened over the Bay of Bengal. The area of reduced convection and anticyclonic anomaly 5 dominate the western North Pacific. Although the southern anticyclonic circulation center 6 has retreated towards the subtropics, circulation 6a has extended farther westward with circulation 5 in the Northern Hemisphere. Over the Northern Hemisphere mid-latitudes, the wave train has evolved such that the cyclonic anomaly 4 has become a trough while the anticyclonic anomaly 7 has intensified over the Gulf of Alaska. The twin cyclonic anomalies 8 and 9 that straddle the equator near the dateline have moved westward between phases 6 and 7.

h. Phase 8

In Figure 10 (bottom), the anticyclonic anomaly 5 and area of reduced convection continue to dominate the western North Pacific. Over the mid-latitudes of both hemispheres, the wave-train patterns have weakened. Over the equatorial central Pacific, twin cyclonic anomalies (8 and 9) straddle the equator with westerly anomalies along the equator. Associated with these circulations is a developing area of enhanced convection near 5°S, 170°E. At this stage, the twin cyclonic anomalies labeled 8 and 9 in Figure 10 (bottom), would evolve as circulations 2 and 3 in phase 1 (Fig. 7 (top)) as the cycle repeats. Also anticyclones 5 and 7 in Fig. 10 (bottom) may be associated with anticyclones 1 and 1b in Fig. 7 (top) as the cycle repeats.

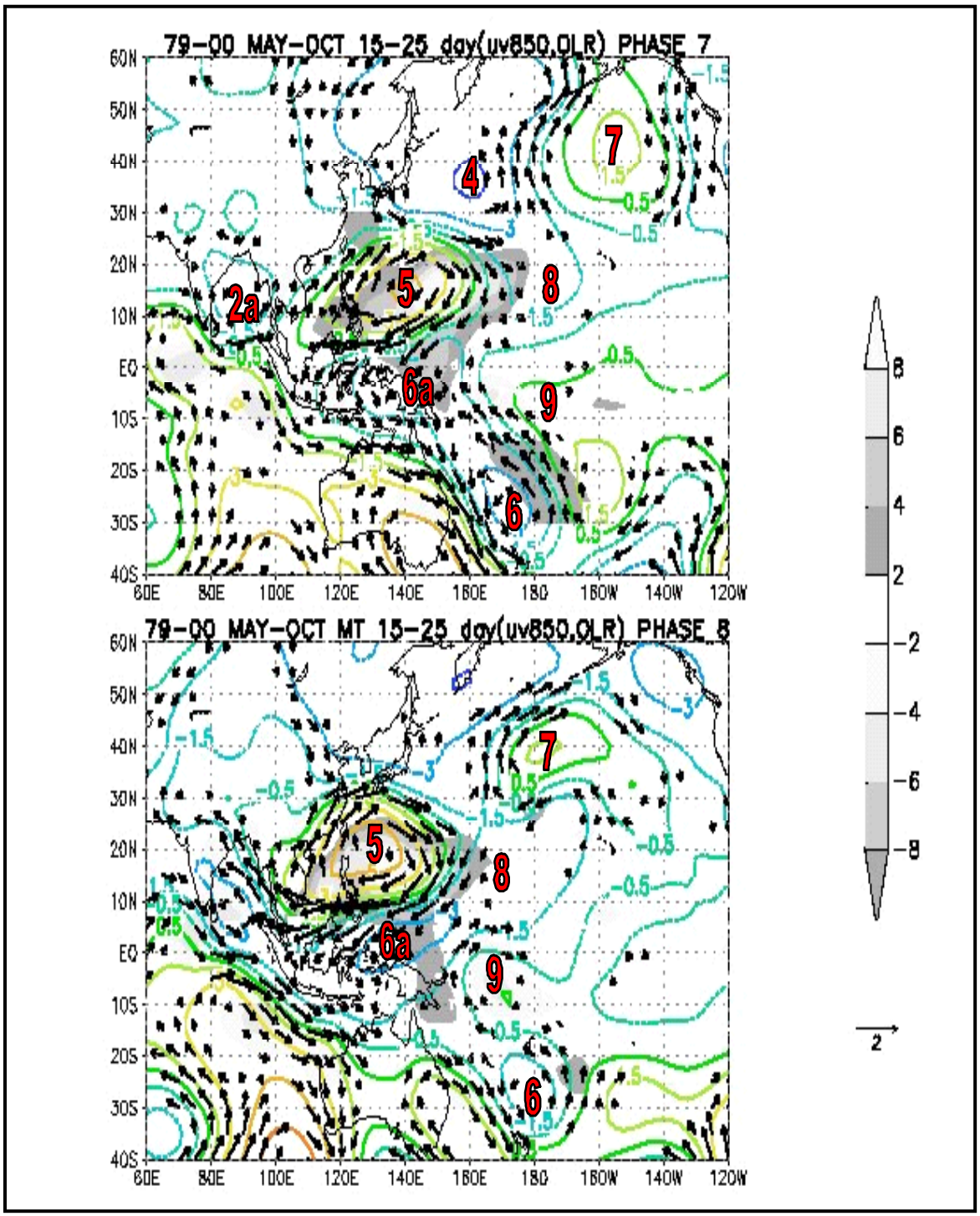

Figure 10. Phases 7 and 8 composites for 850 hPa significant winds (arrows) in m s^{-1} (scale at right), streamfunction (contour interval, 10^6 in m^2 s^{-1}), and OLR (shaded) in W m^{-2}.

The near-equatorial evolution of phases 1 through 8 can be summarized best by examining a Hovmöller diagram (Figure 11) of the 15- to 25-day 850 hPa zonal winds and OLR between 5ºS and 5ºN. Westerly anomalies appear between 5°S and 5°N near 140°E in phase 1. It is important to note that the area of enhanced convection is found east of the maximum westerly anomalies in an area that would have low-level zonal wind convergence. These conditions have been associated with wave energy accumulation (Webster and Chang 1988). The westerly anomalies and area of enhanced convection propagate westward through phase 3, but weaken over the 5°S -5°N latitude band as the cyclonic anomaly (labeled 2 in Figs. 7-10) moves northwestward. However, at phase 4 large easterly anomalies appear over the Indochina Peninsula (80°E-100°E) due to the equatorward extension of anticyclonic anomaly 1b from anticyclonic anomaly 1a in Figs. 7 -10. Meanwhile, easterly anomalies and reduced convection have appeared over the central equatorial Pacific. The pattern of westward-moving easterly anomalies and reduced convection then proceeds through phases 5 through 8.

Therefore, the overall evolution defined by the two leading SVD modes is one of alternating equatorial westerly and easterly zonal winds and associated OLR anomalies propagating westward and northwestward over the western North Pacific. Furthermore, subsequent anomalies tend to appear farther east of previous anomalies (Fig. 11), which is suggestive of an eastward group speed. Therefore, the zonal wind and OLR characteristics defined in Figure 11 are representative of an equatorial Rossby wave pattern. The composite analysis suggests that successive wave features result from perturbations linked to penetration of disturbances that originate as part of the mid-latitude Rossby-wave response to the anomalous circulations over the western North Pacific. Finally, the refraction of the equatorial wave circulations to the northwest coincides with the eastern end of the monsoon-related westerly flow as identified by Takayuba and Nitta (1993) with respect to MRG waves.

As described above and as depicted in Figures 9 and 10, phases 5 through 8 are defined by nearly opposite circulation types to those of phases 1 through 4. Therefore, further analysis of phases 1 through 4 will be described with the understanding that the opposite will be true for the remaining phases.

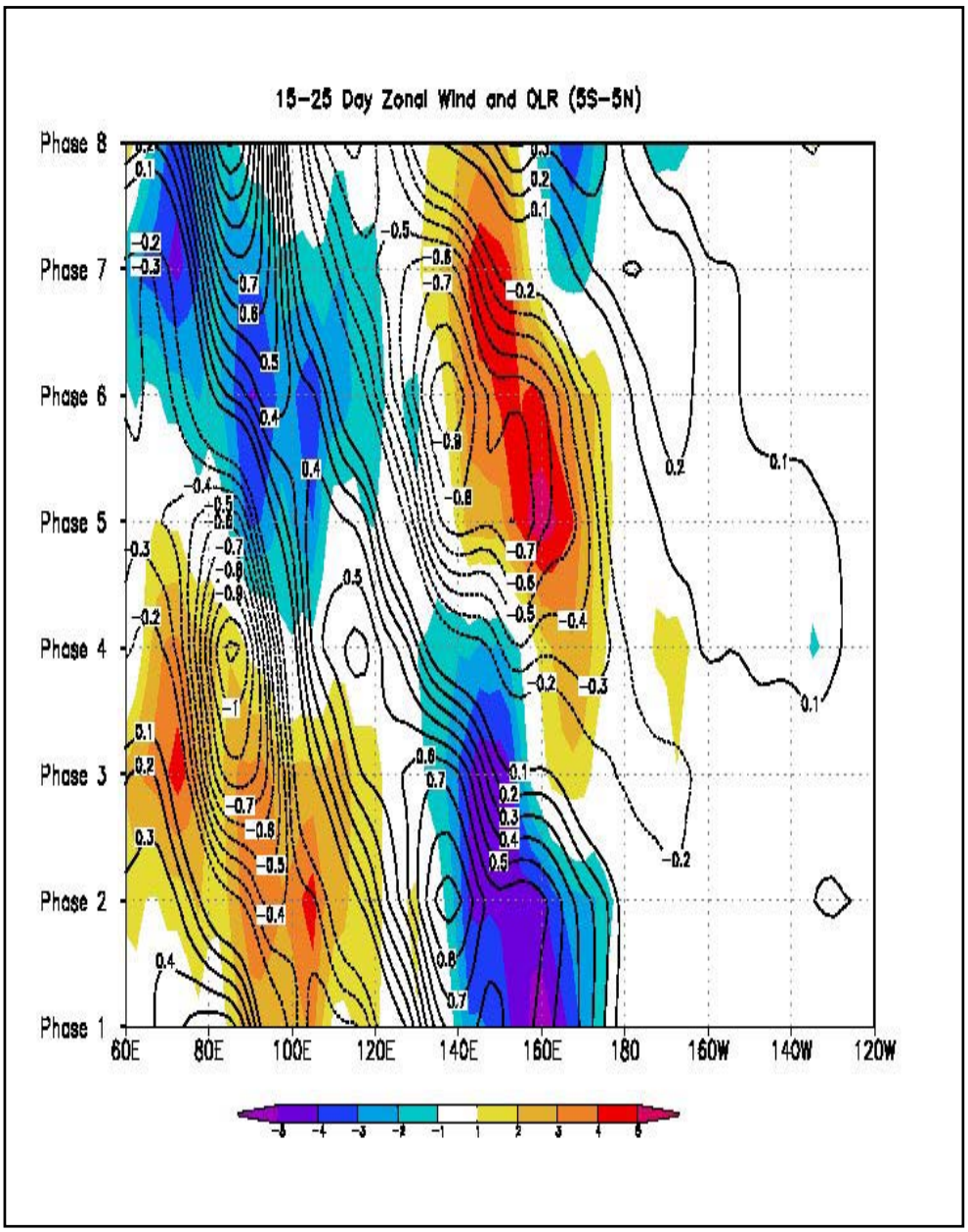

Figure 11. Hovmöller diagram for 15-25 day filtered 850 hPa zonal wind anomalies in m s^{-1} (contours) and 15-25 day filtered OLR anomalies (shaded, see scale at bottom) in W m^{-2}.

2. 850 hPa Heights

Height anomalies at 850 hPa are examined with respect to the numbered circulation anomalies in Figures 7 through 10. Composite plots are displayed such that areas of statistically significant anomalies are shaded.

a. Phase 1

In Figure 12 (top), the maximum positive height anomaly centered just north of the Philippines is associated with the anticyclonic circulation 1 (Fig. 7 (top)). The overall region of higher heights is oriented southwest to northeast with a secondary maximum at 35°N and 170°E that is associated with anticyclonic circulation 1b. The positive anomaly also extends southeast into the Southern Hemisphere across Australia and into the southern mid-latitudes. A small negative anomaly is found west of the positive anomaly along 10°N and 155°E that is associated with cyclonic circulation 2 and a larger negative anomaly is located in the Coral Sea that is associated with circulation 3. A negative height anomaly in the Bering Sea is associated with the trough that extends through the central Pacific to just west of Hawaii.

b. Phase 2

In Figure 12 (bottom), a maximum positive height anomaly is at 33°N, 165°E associated with anticyclonic circulation 1b in Figure 7 (bottom). The entire region of positive height anomalies extends from India in the southwest to the dateline in the northeast. The positive height anomaly associated with anticyclonic circulation 1a has moved westward. The southern negative anomaly associated with cyclonic circulation 3 has deepened while the northern negative anomaly associated with cyclonic circulation 2 has expanded westward. The Southern Hemisphere wave train is evident with a linkage between the negative height anomalies east of Australia and the negative anomalies over the Philippine Sea. Finally, the trough over the central North Pacific has become a closed area of negative height anomalies.

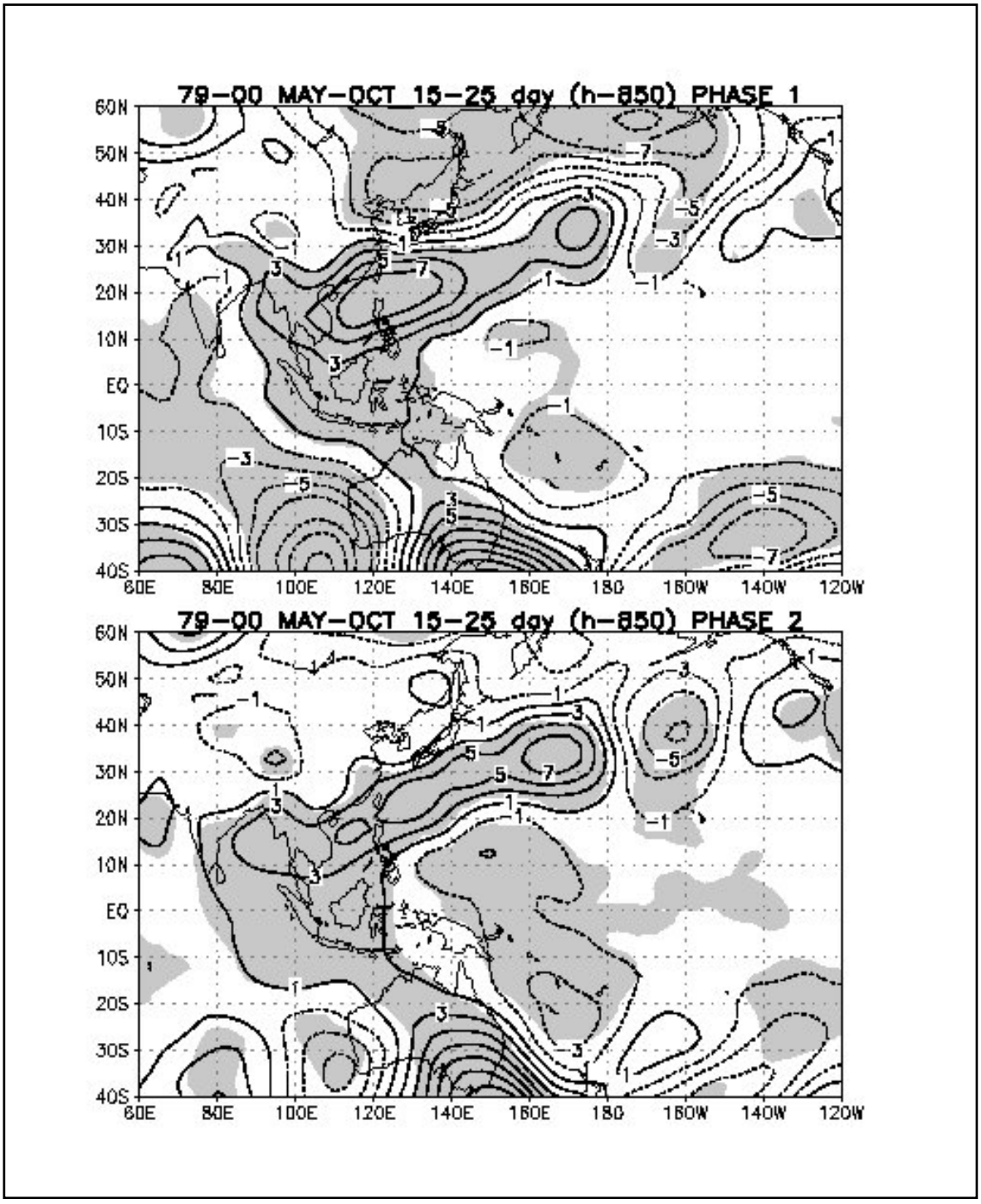

Figure 12. Phases 1 and 2 composites of 850 hPa height anomalies in m with regions of significant height anomalies shaded.

c. Phase 3

In Figure 13 (top), the large area of positive heights associated with anticyclonic circulation 1 has split such that the southern branch moves westward with a maximum in the Bay of Bengal that is associated with anticyclonic circulation 1a and the second maximum associated with anticyclonic circulation 1b that moves northwest to the east of Japan. The negative height anomaly associated with cyclonic circulation 2 has moved westward to 140°E and deepened. This negative anomaly extends southeastward into the Southern Hemisphere in association with cyclonic circulations 3a and 3b.

d. Phase 4

In Figure 13 (bottom), the negative height anomaly associated with cyclonic circulation 2 extends from Indonesia northeast into the Gulf of Alaska. The linkage with the Southern Hemisphere mid-latitude wave train has been broken. However, negative anomalies that are associated with the Southern Hemisphere cyclonic anomalies 3 and 3a remained loosely coupled to circulation 2.

The evolution of positive and negative height anomalies in phases 1 through 4 in Figures 12 and 13 is consistent with the primary anticyclonic and cyclonic circulation anomalies defined in Figures 7-8. However, the development of anticyclonic anomalies 5 and 6 over the sub-tropical latitudes of the central North and South Pacific is not evident in the height anomaly fields. The development in phases 5 through 8 (not shown) are similar, but with opposite circulation types. In all phases, the height anomalies are geostrophically consistent with the circulation anomalies, with only small height anomalies along the equator.

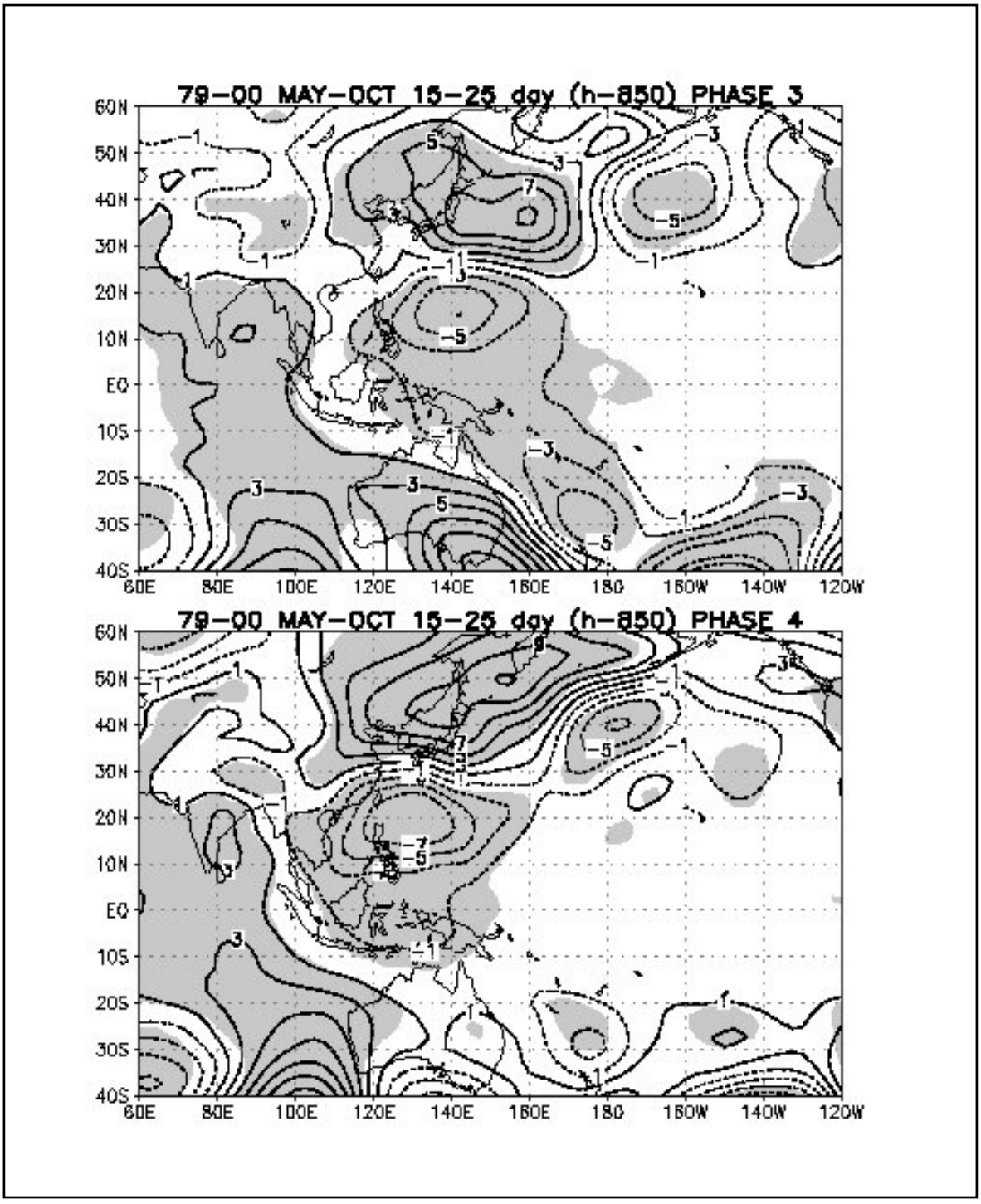

Figure 13. Phases 3 and 4 composites of 850 hPa height anomalies in m with regions of significant height anomalies shaded.

3. 500 hPa Heights

The 500 hPa height anomalies during phase 1 (Fig. 14 (top)), phase 2 (Fig. 14 (bottom)), phase 3 (Fig. 15 (top)), and phase 5 (Fig. 15 (bottom)) are examined as they provide a clear representation of the origin of the cyclonic anomaly 2 in Figure 7 and the anticyclonic anomalies 5 and 6 in Figures 8 and 9.

a. Phase 1

In phase 1, the positive height anomaly over the East China Sea that extends to the central North Pacific in Figure 14 (top) is clearly associated with anticyclonic anomaly 1 in Figure 7 (top). During this phase, a small area of negative height anomalies appears near 10°N, 160°E at the base of the anomalous trough in Figure 7 (top) that extends equatorward from the Gulf of Alaska. A corresponding negative height anomaly occurs at 20°S, 160°E as the most equatorward extension of trough 3 in the Southern Hemisphere wave train.

b. Phase 2

In phase 2 (Fig. 14 (bottom)), the height anomalies over the central Pacific have become more negative with pronounced connection to the mid-latitude cyclonic circulation. Therefore, there appears to be a relation between the mid-latitude and tropical circulation anomalies such that the Northern Hemisphere negative height perturbation at 10°N is due to equatorward penetration of a disturbance related to the mid-latitude wave that had emanated earlier from the anomalous reduced convection over the western North Pacific (circulation 1). The Southern Hemisphere anomaly phases with the equatorward penetration of a trough in the mid-latitude wave pattern.

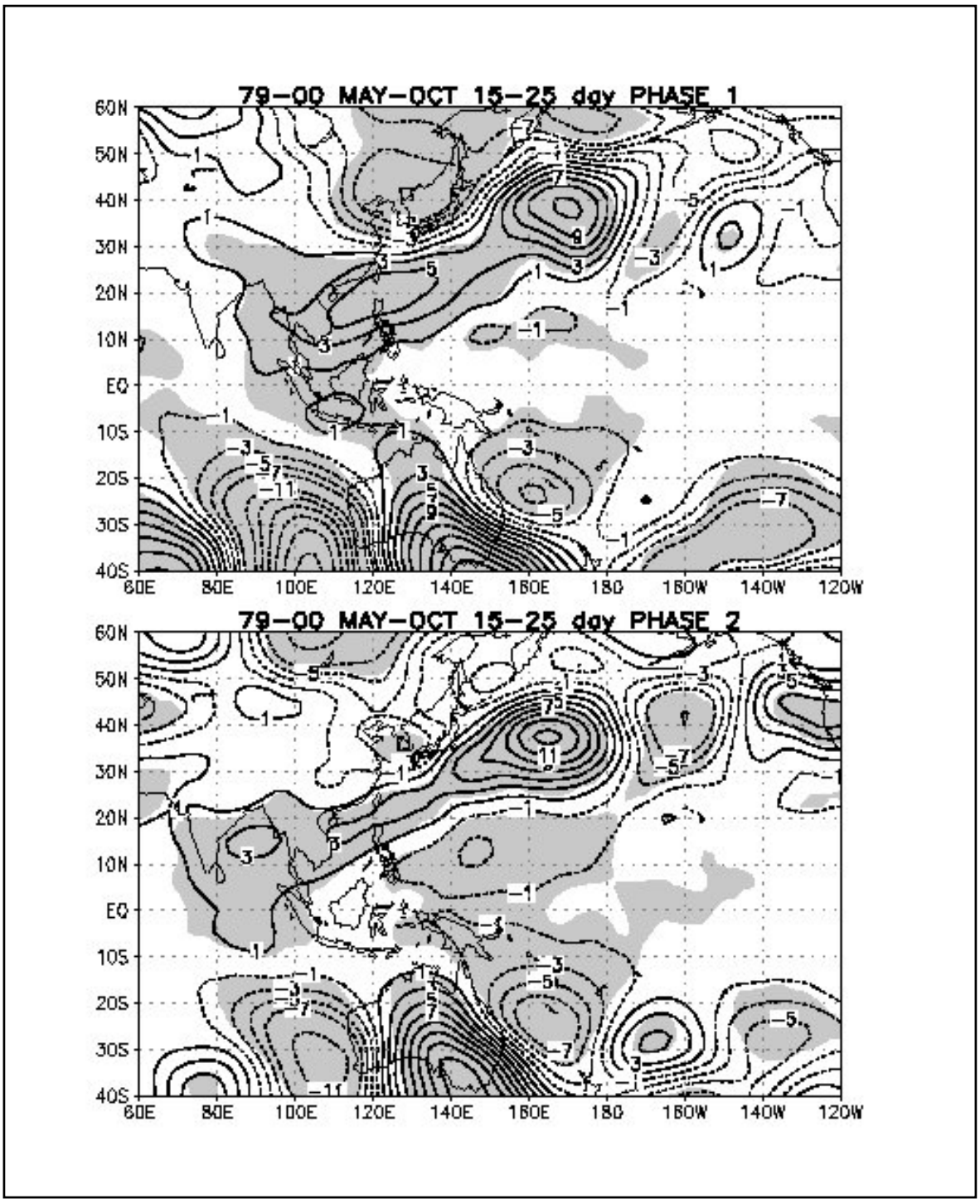

Figure 14. Phases 1 and 2 composites of 500 hPa height anomalies in m with regions of significant height anomalies shaded.

c. Phases 3 and 5

During phase 3, the anomalous cyclonic anomaly 2 (Fig. 8) and the area of negative height anomalies (Fig. 15 (top)) amplifies and moves eastward over the Philippine Sea. Although a linkage remains with the Southern Hemisphere via circulation 3a (Fig. 8) and its associated negative height anomalies (Fig. 15 (top)), the connection between the anomalous cyclone and negative height anomaly of circulation 4 has been broken. During this phase, a ridge extends equatorward from anticyclone 1b (Fig. 8) with positive height anomalies near 20ºN, 170ºW.

The evolution from phase 3 through phase 5 is such that the northern mid-latitude wave pattern shifts westward and the subtropical anticyclonic anomaly 5 and positive height anomaly have connected to an anticyclone and positive height anomaly near 30ºN, 165ºW. The evolution of the anticyclone 5 and positive height anomalies at 15ºN, 160ºE and 20ºS, 160ºE evolve as the cyclonic anomalies 2 and 3 (Figs. 7 and 8) and negative height anomalies during phases 1 and 2 (Fig. 14).

Thus, the evolution of successive circulation anomalies over the sub-tropical latitudes of both hemispheres is evident in the low-level wind anomalies and mid-level height anomalies.

4. 850 hPa Temperatures

a. Phase 1

In Figure 16 (top), low-level temperature anomalies are dominated by mid-latitude circulation patterns. The Southern Hemisphere wave train is evident, especially for the cold anomaly associated with the anomalous trough east of Australia. Weak positive temperature anomalies over the South China Sea are related to the anticyclonic anomaly 1 in Figure 7 (top) and areas of reduced convection. This region extends from Singapore to the northeast towards the Gulf of Alaska with a minimum at 32°N, 170°W related to anticyclonic circulation 1b.

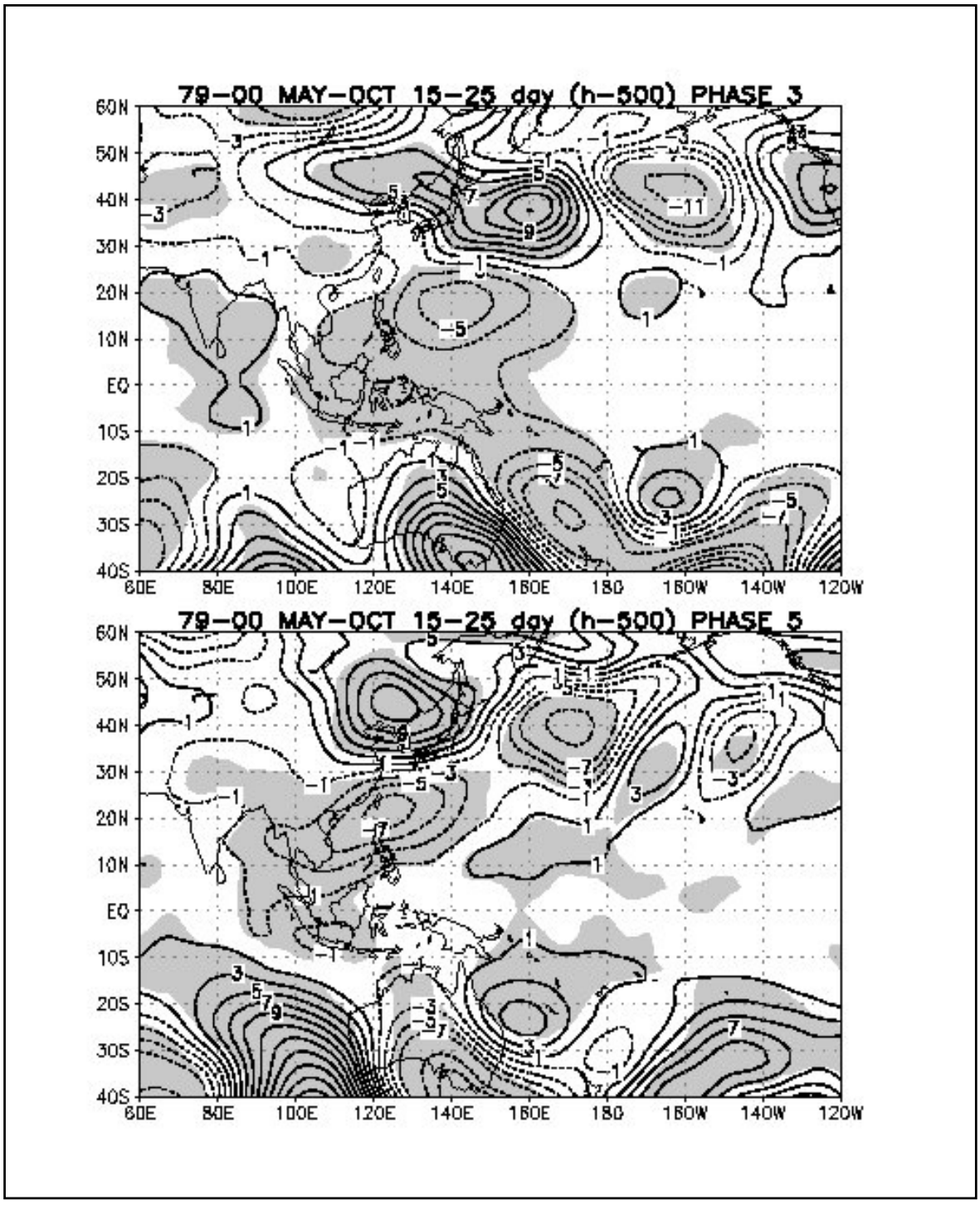

Figure 15. Phases 3 and 5 composites of 500 hPa height anomalies in m with regions of significant height anomalies shaded.

b. Phase 2

In Figure 16 (bottom), the negative temperature anomaly east of Australia is associated with the cyclonic anomaly 3 in Figure 7 (bottom). A negative anomaly is also found at 5°N, 130°E that is associated with the cyclonic anomaly 2 (Fig. 7 (bottom)) and southwesterly flow with enhanced convection. The large positive anomaly region associated with anticyclonic circulation 4 near 40°N, 170°W moves westward and extends into the subtropics.

c. Phase 3

In Figure 17 (top), the negative temperature anomaly over Eastern Australia associated with cyclonic circulations 3a and 3 intensifies and extends farther to the northwest. The negative anomaly in the equatorial western Pacific associated with cyclonic circulation 2 has moved northward.

d. Phase 4

In Figure 17 (bottom), the temperature anomaly pattern associated with the Southern Hemisphere wave train has become disorganized as the wave pattern has weakened (Fig. 8 (bottom)). Small negative anomalies over the western North Pacific are associated with cyclonic circulation 2 (Fig. 8 (bottom)). Small warm anomalies begin to appear in the equatorial central Pacific and are associated with the anticyclonic anomalies that appear in phase 5 (Fig. 9 (top)).

Therefore, these overall temperature anomalies at low levels are generally consistent with the circulation height anomalies. At the mature stage with respect to the region of enhanced convection over the Philippine Sea, the temperature anomaly pattern became somewhat disorganized, which may be due to the large spatial extent of deep convection.

Temperature anomaly patterns indicate a connection between significant equatorial anomalies and mid-latitude anomalies in both hemispheres. Again, this is consistent with the associated circulation and height anomaly composites.

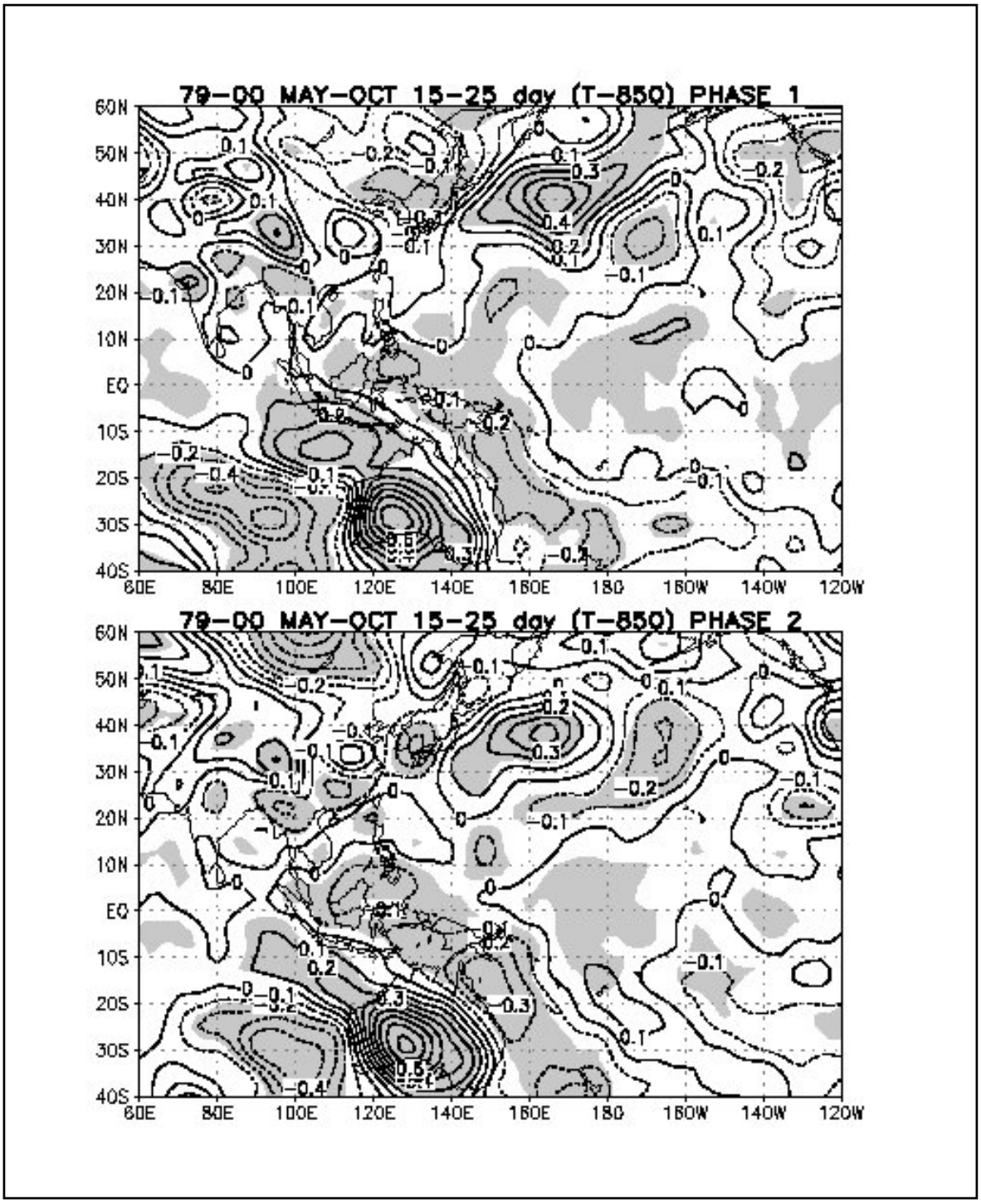

Figure 16. Phases 1 and 2 composites for 850 hPa temperature anomalies in °C, negative (dashed contours), positive (solid contours) with significant temperature anomalies shaded.

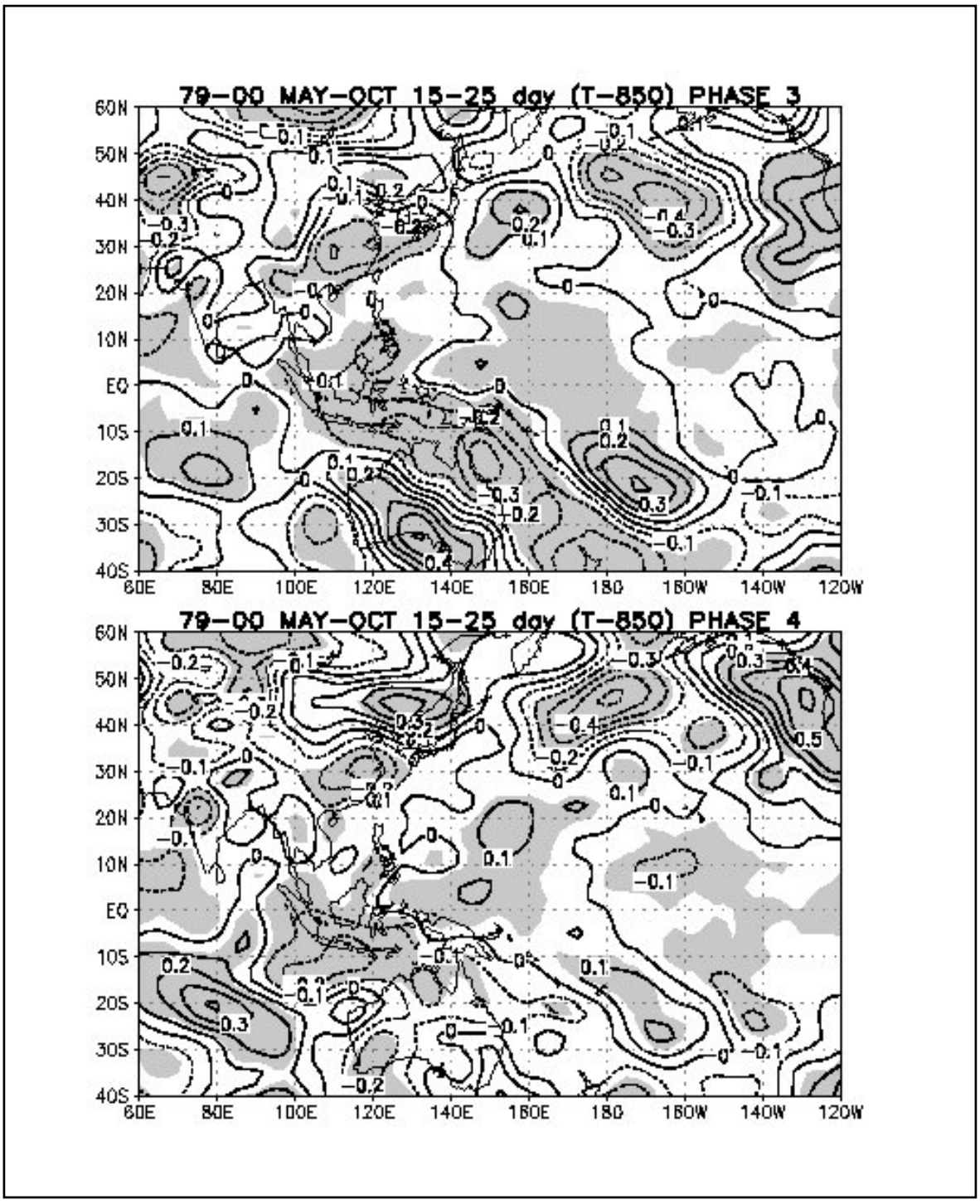

Figure 17. Phases 3 and 4 composites for 850 hPa temperature anomalies in °C, negative (dashed contours), positive (solid contours) with significant temperature anomalies shaded.

5. OLR and 200 hPa Winds

a. Phase 1

In Figure 18 (top), a large 200 hPa cyclonic anomaly in the western North Pacific is associated with the low-level anticyclonic anomaly 1 in Figure 7 (top). The combination of the large cyclonic anomaly over the western North Pacific and a cyclonic anomaly in the Southern Hemisphere at 20°S, 170°E contributes to strong southeasterly anomalies that are associated with the area of reduced convection over the western North Pacific. The Southern Hemisphere cyclonic anomaly is part of a well-defined wave-train that follows an arc-type path that originates west of Australia and curves cyclonically to the central South Pacific. The cyclonic anomaly at 20ºS, 170ºE represents the most equatorward extension of the wave train. This wave train pattern is similar to that defined by Straub and Kiladis (2003a) in association with the extratropical forcing of Kelvin wave activity over the equatorial central Pacific.

b. Phase 2

In Figure 18 (bottom), the 200 hPa cyclonic anomaly that is associated with the reduced convection over the western North Pacific has moved westward and weakened. The flow from the Southern Hemisphere has been reduced such that only the flow from the cyclonic anomaly west of Australia contributes to the main region of reduced convection. The cyclonic anomaly east of Australia has retreated toward the mid-latitudes as the mid-latitude wave train has progressed and retreated poleward. A partial Rossby-wave pattern is evident across the North Pacific, but it is not as well defined as at lower levels (Fig. 7 (bottom)).

c. Phase 3

In Figure 19 (top), the 200 hPa cyclonic anomaly associated with the extreme western North Pacific region of reduced convection has continued to weaken. As the region of enhanced convection begins to spread over the western North Pacific, upper-level anticyclonic anomalies have extended over the Philippine Sea. The cyclonic anomaly east of Australia has weakened and has moved eastward with the progression of the mid-latitude wave pattern.

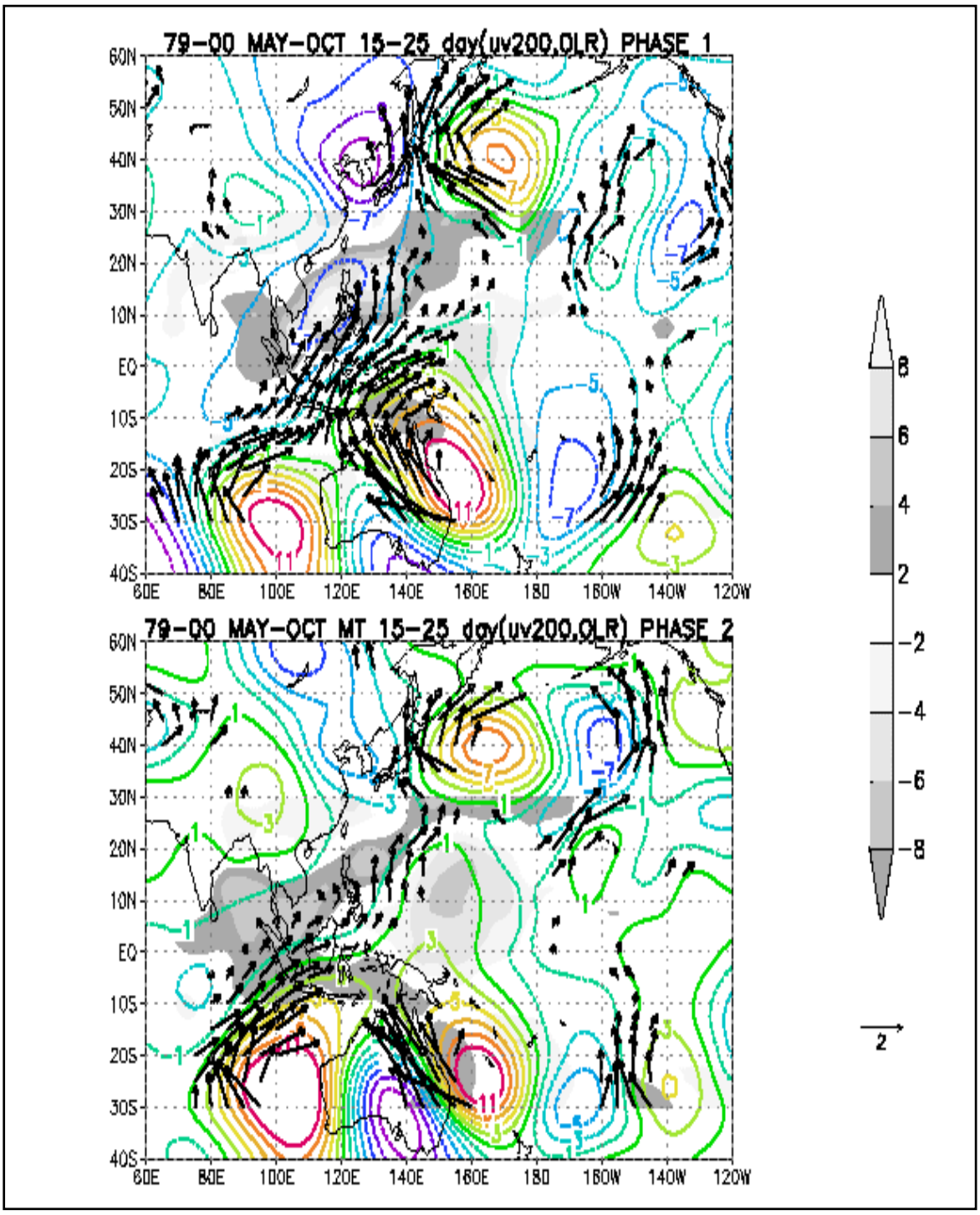

Figure 18. Phase 1 and 2 composites for 200 hPa winds (arrows) in m s^{-1} (scale at right), streamfunction (contours) in m^2 s^{-2}, and OLR (shaded) in W m^{-2}.

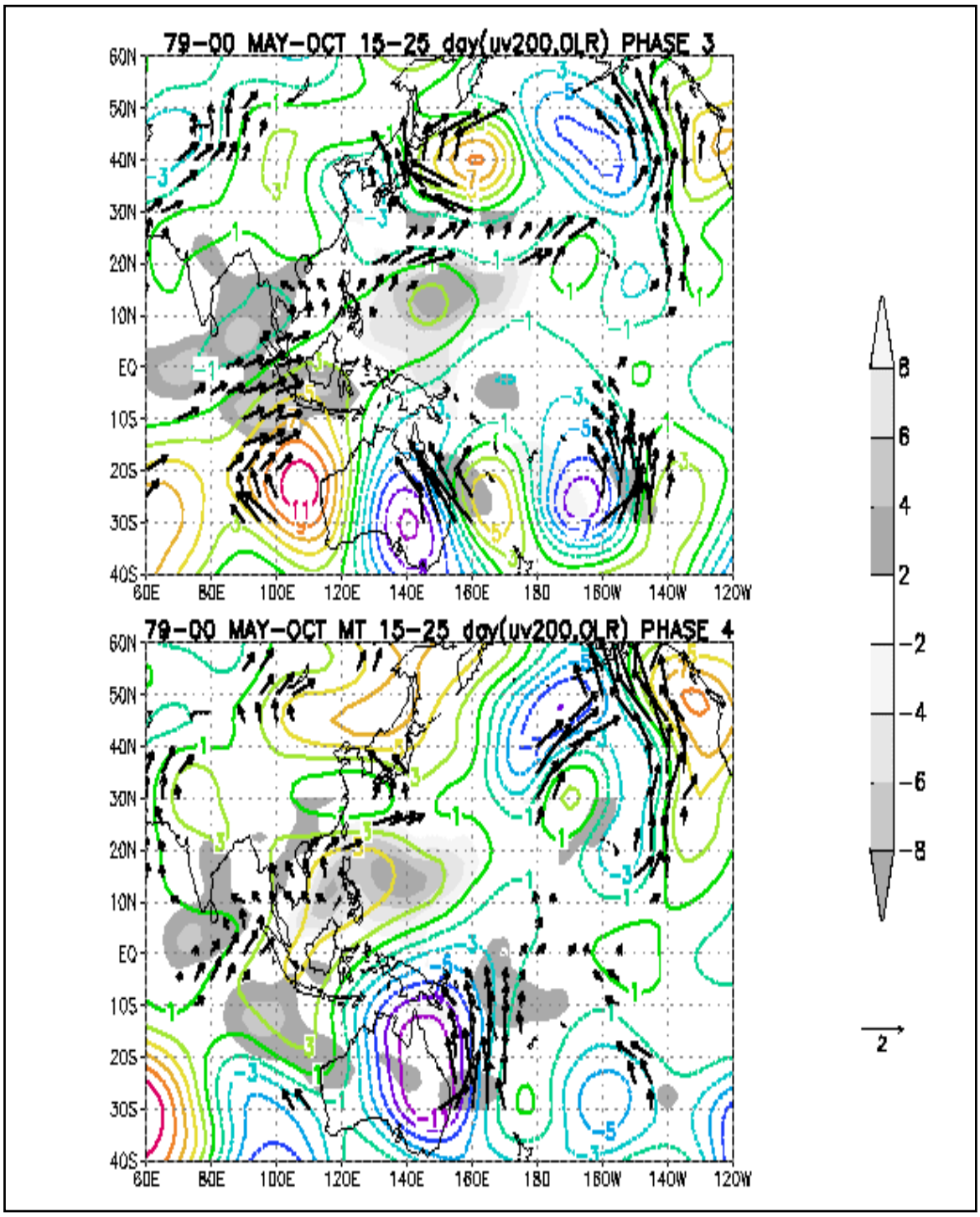

Figure 19. Phases 3 and 4 composites for 200 hPa winds (arrows) in m s^{-1} (scale at right), streamfunction (contours) in m^2 s^{-2}, and OLR (shaded) in W m^{-2}.

d. Phase 4

In Figure 19 (bottom), the dominant pattern is one of 200 hPa anticyclonic anomalies over the western North Pacific associated with the low-level cyclonic anomaly 2 (Fig. 8 (bottom)) and enhanced convection. Furthermore, the Southern Hemisphere wave pattern has progressed such that a large anticyclonic anomaly is present over eastern Australia.

Therefore, the upper-level anomalies evolve as a combination of the progression of a Southern Hemisphere mid-latitude wave pattern that penetrates equatorward in conjunction with anomalies over the western North Pacific that are related to the alternation between reduced and enhanced convection. Also, the combination of lower and upper-level anomalies over the western North Pacific are such that the circulations have a baroclinic structure with an upper-level anticyclone over a low-level cyclone during periods of enhanced convection, while opposite conditions exist during periods of reduced convection. The mid-latitude wave pattern in the Southern Hemisphere has an equivalent barotropic structure. These structural characteristics are consistent with the response of the tropical atmosphere to centers of diabatic forcing (Webster and Chang 1988, Wang and Xie 1996).

Finally, the circulation characteristics at low levels over the western North Pacific and into the Northern Hemisphere mid-latitudes seem better defined at low levels than at upper levels. This is consistent with the analysis of Wang and Xie (1996) for the case of easterly vertical wind shear, which is the climatological condition over the western North Pacific during the Northern summer. In that case, the baroclinic and barotropic modes of the Rossby response to equatorial heating align such that they cancel at upper levels and reinforce at low levels.

Similar analyses of composite variables, which included temperature, relative humidity, and vertical motion (omega), were conducted. Because these results were consistent with the above discussions, they will not

be shown. In particular, the relative humidity and vertical motion anomalies were very consistent to the OLR anomalies, which is an important validation of the two independent data sets.

C. VARIABILITY DUE TO THE LARGE-SCALE BASIC STATE OF THE ATMOSPHERE

In response to latent heat release over areas of tropical deep convection, the atmosphere responds as a series of large-scale waves that propagate horizontally and penetrate vertically throughout the troposphere. The response is in the form of Kelvin waves to the east and Rossby waves to the west of the heat source (Gill 1980). Many of the circulation characteristics defined with respect to the composites in section B resemble the forced response to tropical heating. In particular, the character of the alternating anticyclonic circulation (1 on Fig. 7) and cyclonic circulation (2 on Fig. 8) resembles a Rossby-wave response from the regions of reduced and enhanced convection. Furthermore, Rossby wave trains appear to emanate from tropical heat sources (Hoskins and Karoly 1981) to the mid-latitudes. The structure of the Rossby waves is baroclinic near the heat source and equivalent barotropic away from the heat source (Webster 1972). If there is no vertical variation in the mean state, the equivalent barotropic mode will have small amplitude (Lim and Chang 1983). If there is vertical shear, it will contribute to the transfer of energy from the internal (baroclinic) mode to the external (barotropic) mode and thereby extract energy from the tropics and transport it to the extratropics (Wang and Xie 1996). Wang and Xie (1996) demonstrated that the character of the forced wave response is different between basic states with easterly and westerly vertical shear. In an easterly shear environment, the Rossby wave response is confined to the lower troposphere, which is consistent with the composite patterns in Figures 7 through 10. Because the typical basic state over the tropical western Pacific during northern summer is one of easterly vertical shear, this is a dominant part of the large-scale 15- to 25-day circulation signal, which was identified by the SVD analysis.

In a study of upper-level wave activity over the Pacific, Arkin and Webster (1985) found a maximum in perturbation kinetic energy (PKE) in the mean

westerlies but maximum convection occurred in the easterlies at a longitude to the east of the longitude of the maximum westerlies. Therefore, the energy source for the PKE in the westerlies must be remote and transferred from an area of easterlies. Webster and Chang (1988) examined the accumulation of wave energy that could be transferred to the region of maximum PKE in terms of the confluence of westerly zonal wind over equatorial latitudes. In regions of confluence where the zonal wind decreases to the east, wave energy is accumulated and then made available for poleward transfer to regions of westerly flow. Although the arguments of Webster and Chang (1988) are applied to the upper-level flow over the Pacific during the northern winter, similar conditions apply in the low-level monsoon flow of the northern summer over the equatorial western Pacific. Convergence of equatorial zonal flow contributes to the contraction of the zonal wavelength of a Rossby wave such that the phase speed minus the group velocity equals zero (Webster and Chang 1988). This results in an energy accumulation to the east of the westerly maximum in zonal winds. Thus, energy accumulation is not in phase with the westerly maximum.

Wang and Xie (1996) examined the role of vertical shear in energy accumulation and Rossby wave emanation in regions of upper-level westerly ducts and the low-level monsoon trough. They formulated a two-level model on an equatorial plane such that the governing equations were written in terms of two vertical (one barotropic and one baroclinic) modes. Their first experiment was based solely on the meridional cyclonic shear of the zonal wind without vertical shear. Their results showed that meridional shear alone had little impact on the two modes as the barotropic and baroclinic modes remain decoupled while the barotropic mode develops into the form of a non-divergent Rossby wave. Their second experiment included both meridional zonal shear and vertical shear (easterly and westerly). In the case of easterly shear, the baroclinic and barotropic modes were nearly out of phase, which confines wave perturbations to the lower levels. In the presence of westerly shear, the baroclinic mode acts to force the barotropic mode. Therefore, the purpose of this

section is to examine the variations in the composite patterns of section B relative to changes in vertical shear and confluence/diffluence of the zonal wind.

a. Vertical Wind Shear

In an easterly shear environment, low-level equatorial westerly winds extend eastward through the Philippine Sea to 150ºE (Fig. 20 (top)), while 200 hPa easterlies cover the majority of the equatorial western Pacific (Fig. 21 (top)). When the environment is one of westerly vertical shear, 850 hPa westerlies only extend eastward through the South China Sea (Fig. 20 (bottom)) while the eastward extent of the upper-level easterlies is reduced (Fig. 21 (bottom)). The tropical upper-tropospheric trough (TUTT) is enhanced. In 50 of the 63 cases that were used to construct the composites of 15- to 25- day variability, easterly shear existed, and the remaining 13 cases were westerly shear environments. Because of the small percentage of occurrences of westerly shear environments, only cases of easterly shear environments will be examined. Furthermore, a westerly shear basic state is less favorable for tropical cyclone activity than is easterly shear, so an insufficient sample of tropical cyclones would have been available for the westerly shear cases.

b. Easterly Vertical Shear and Low-Level Zonal Convergence and Divergence

During phase 1 (Fig. 7 (top)), the equatorial cyclonic anomaly and area of enhanced convection have just entered the equatorial western Pacific. Therefore, it is assumed that the character of the basic state during phase 1 may dictate the evolution of the entire 15- to 25- day pattern.

The zonal winds for easterly vertical shear cases were examined for cases of convergence (Fig. 22 (top)) and divergence (Fig. 22 (bottom)) within an area from the equator to 10°N between 140°E and 160°E. Convergence is found in this region because the maximum in equatorial westerlies is at 140°E and easterlies exist from 160ºE eastward. For divergent cases, equatorial westerlies penetrate to the dateline with a local westerly wind maximum occurring over the eastern portion of the region (near 155°E). Given that this 10ºN, 140ºE-160ºE, this region has divergence. This eastward

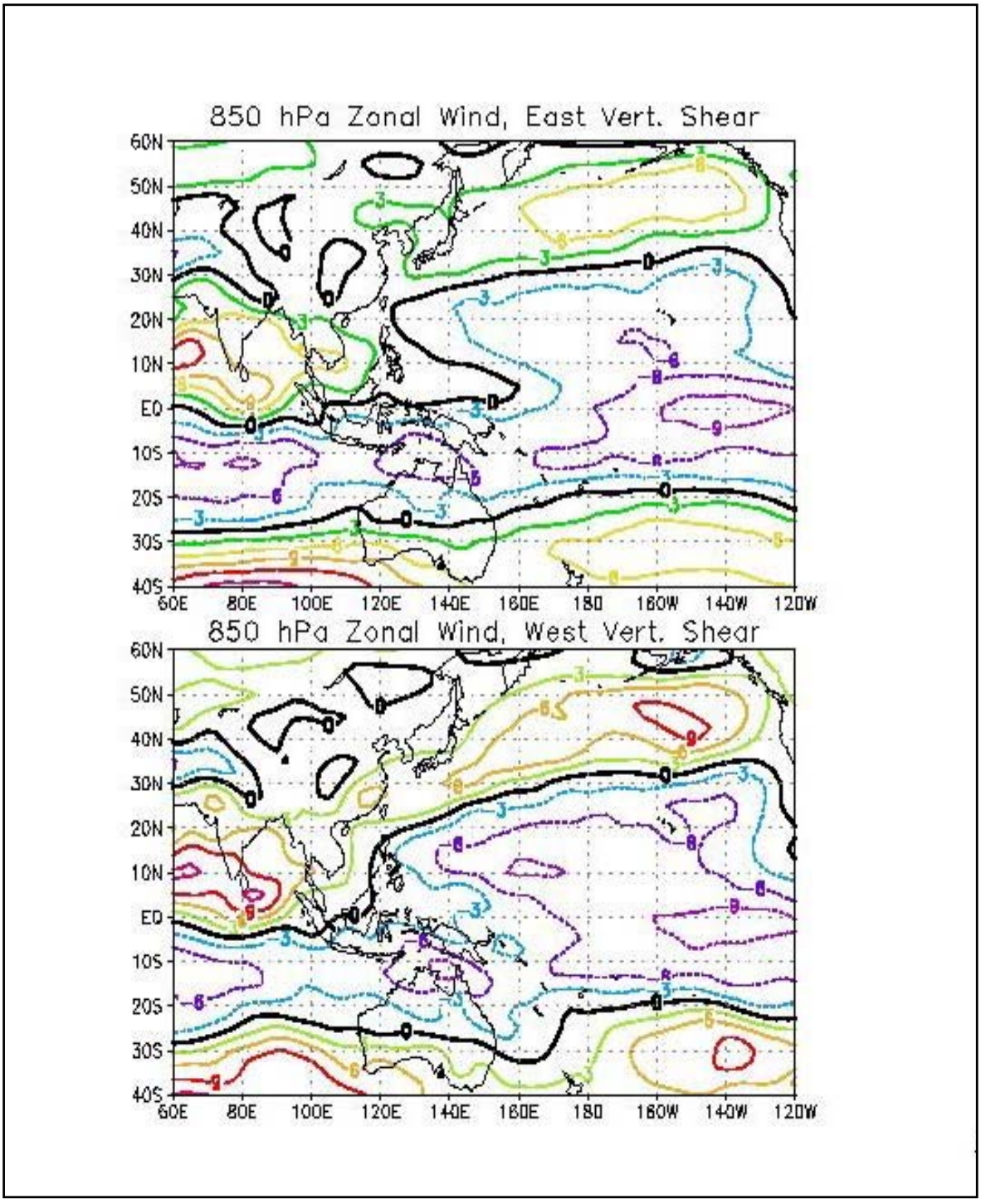

Figure 20. Average 850 hPa total zonal wind (m s^{-1}) with (top) easterly vertical wind shear and (bottom) westerly vertical wind shear.

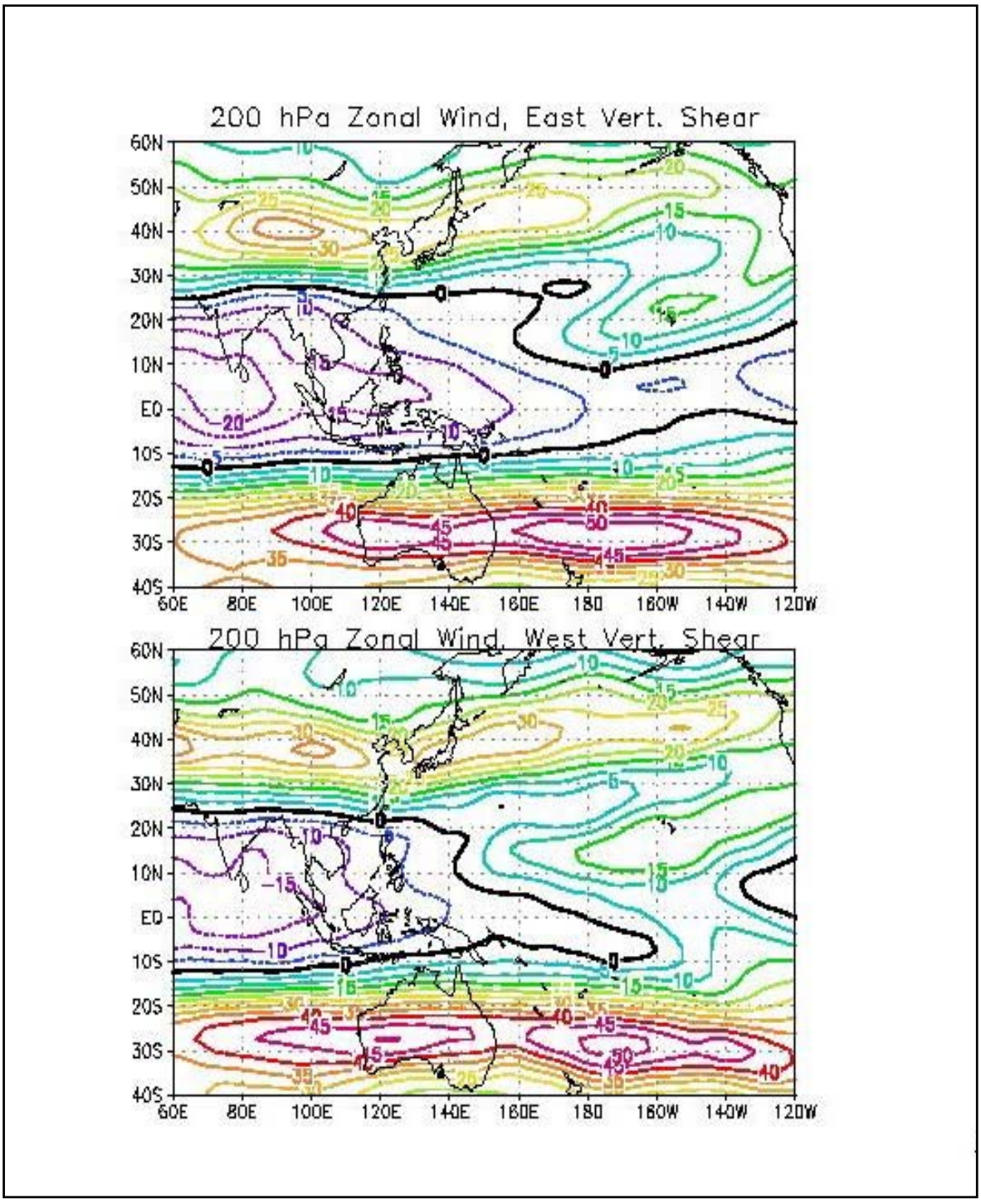

Figure 21. Average 200 hPa total zonal wind (m s^{-1}) for phase 1 and (top) easterly vertical wind shear and (bottom) westerly vertical wind shear.

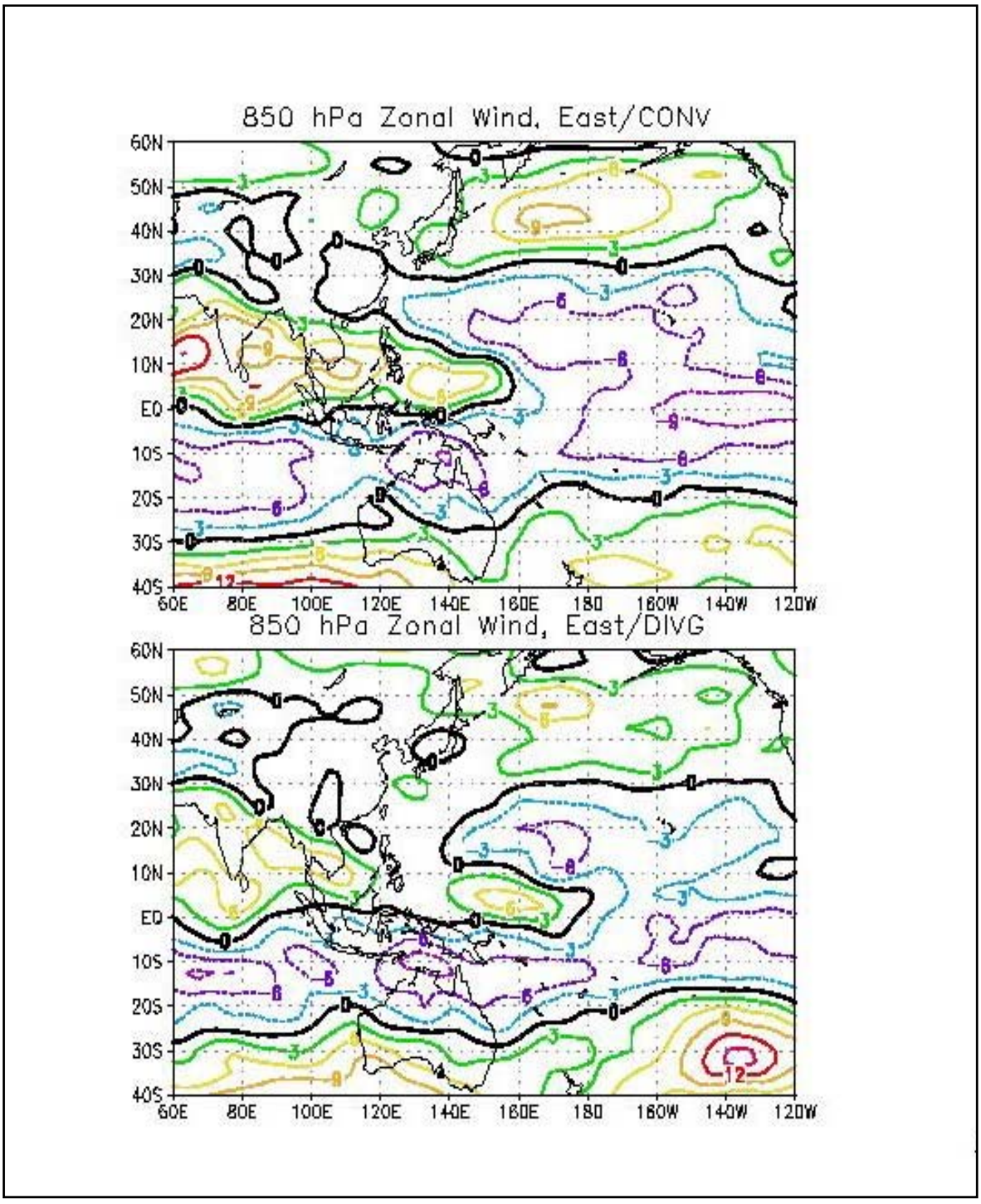

Figure 22. Average 850 hPa total zonal wind (m s^{-1}) with easterly vertical wind shear, and (top) zonal wind convergence and (bottom) zonal wind divergence. Divergence and convergence are defined over a region Equator – 10ºN and 140ºE-160ºE.

penetration of the equatorial westerlies is similar to that of an El Niño (Rasmussen and Carpenter 1982).

The objective is to demonstrate that variations exist between the circulation patterns for the subsets of cases with zonal wind convergence versus zonal wind divergence. Only phases 1 and 2 will be compared for each case. Then these different patterns will be related to differences in tropical cyclone activity (especially formation locations) in the following section.

c. Composites for Cases of Zonal Convergence

The evolution of the 15-25 day pattern during periods of easterly shear and zonal convergence is similar to the overall composites in Figures 7 through 10 because 33 of the 50 cases fall into this category.

During phase 1 of the easterly shear and zonal convergence cases (Fig. 23 (top)), the anticyclone over the South China Sea and the East China Sea is oriented southwest to northeast and appears to be connected to the Northern Hemisphere mid-latitude wave train. A cyclone is found to the southeast over the Philippine Sea. The Southern Hemisphere mid-latitude wave train appears to interact with the equatorial waves in the tropics.

During phase 2 (Fig. 23 (bottom)), the cyclone has intensified over the Philippine Sea. A cyclone in the Southern Hemisphere mid-latitudes appears to be connected to the enhanced convection region. The wave train over the Northern Hemisphere mid-latitudes appears to develop more fully throughout the eastern North Pacific near 150°W.

The equatorward extension of a ridge from the anticyclonic anomaly at 35ºN, 165ºW contributes to the development of the next cell in the equatorial Rossby-wave pattern. Of importance in these composites with zonal wind convergence is the contraction of the cyclonic anomaly at 10ºN, 140ºE and refraction northwestward away from the equator as it interacts with the convergence at the eastern end of the monsoon westerly flow.

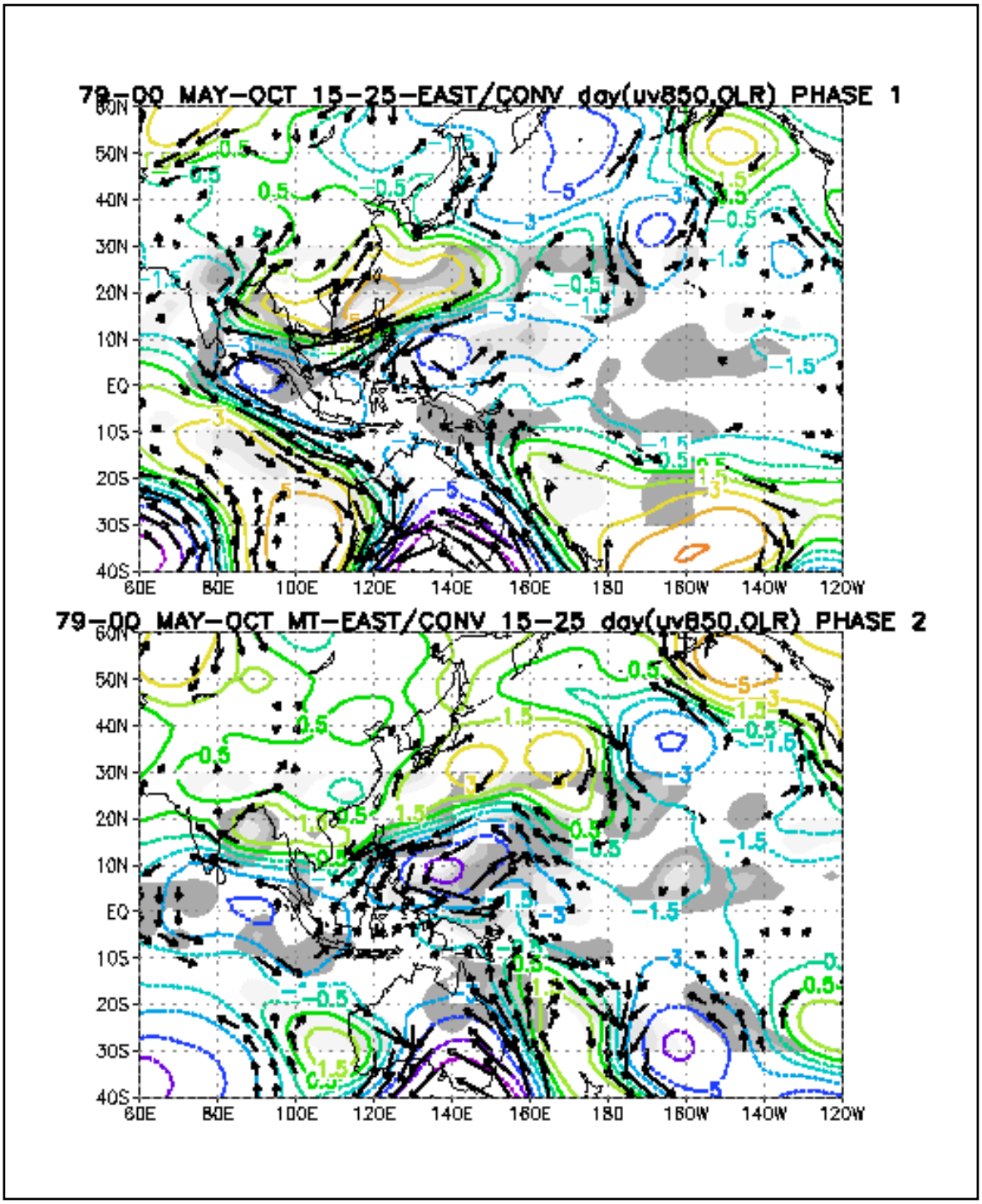

Figure 23. Same as in Fig. 7, except cases when there was easterly shear and zonal convergence.

d. Composites for Cases of Zonal Divergence

Although there is divergence over the target region equator-10ºN, 140ºE-160ºE, anomalous convergence of the zonal winds is then shifted farther east in association with the local maximum in westerly winds that is now near the dateline (Fig. 20 (bottom)). When the divergent condition exists (Fig. 24 (top)), the anticyclone north of the Philippines during phase 1 appears somewhat similar to the composite with zonal convergence (Fig. 23 (top)). However, the cyclonic anomaly that is southeast of the anticyclonic anomaly is now shifted to the dateline in the zonal divergence composite (Fig. 24 (top)). More importantly, the wave train into the Northern Hemisphere mid-latitudes is clearly connected with this cyclonic anomaly near the dateline. The wave train is also much more pronounced than in the zonal wind convergence composite (Fig. 23 (top)).

During phase 2 (Fig. 24 (bottom)), the anomalous cyclone at 10ºN, 150°E has intensified. The cyclonic anomaly has developed a more zonal orientation relative to phase 1. There also appears to be less interaction with the Southern Hemisphere mid-latitude wave train. The next anticyclonic circulation to appear in the cycle develops near 140ºW as a ridge extension into the eastern Pacific from the mid-latitude wave train.

Therefore, the westward-moving cyclonic anomaly at 10ºN, 180º in phase 1 interacts with the local maximum in westerly winds but then experiences local divergence near 160ºE. This results in less contraction in the zonal wavelength and reduced refraction away from the equator. Rather, Rossby-wave emanations from the central equatorial Pacific appear to be more intense than the wave emanation from the western North Pacific during zonal convergence cases. Furthermore, the Northern Hemisphere mid-latitude wave train and subsequent development of equatorial disturbances are all farther east than the zonal convergence case in Figure 23.

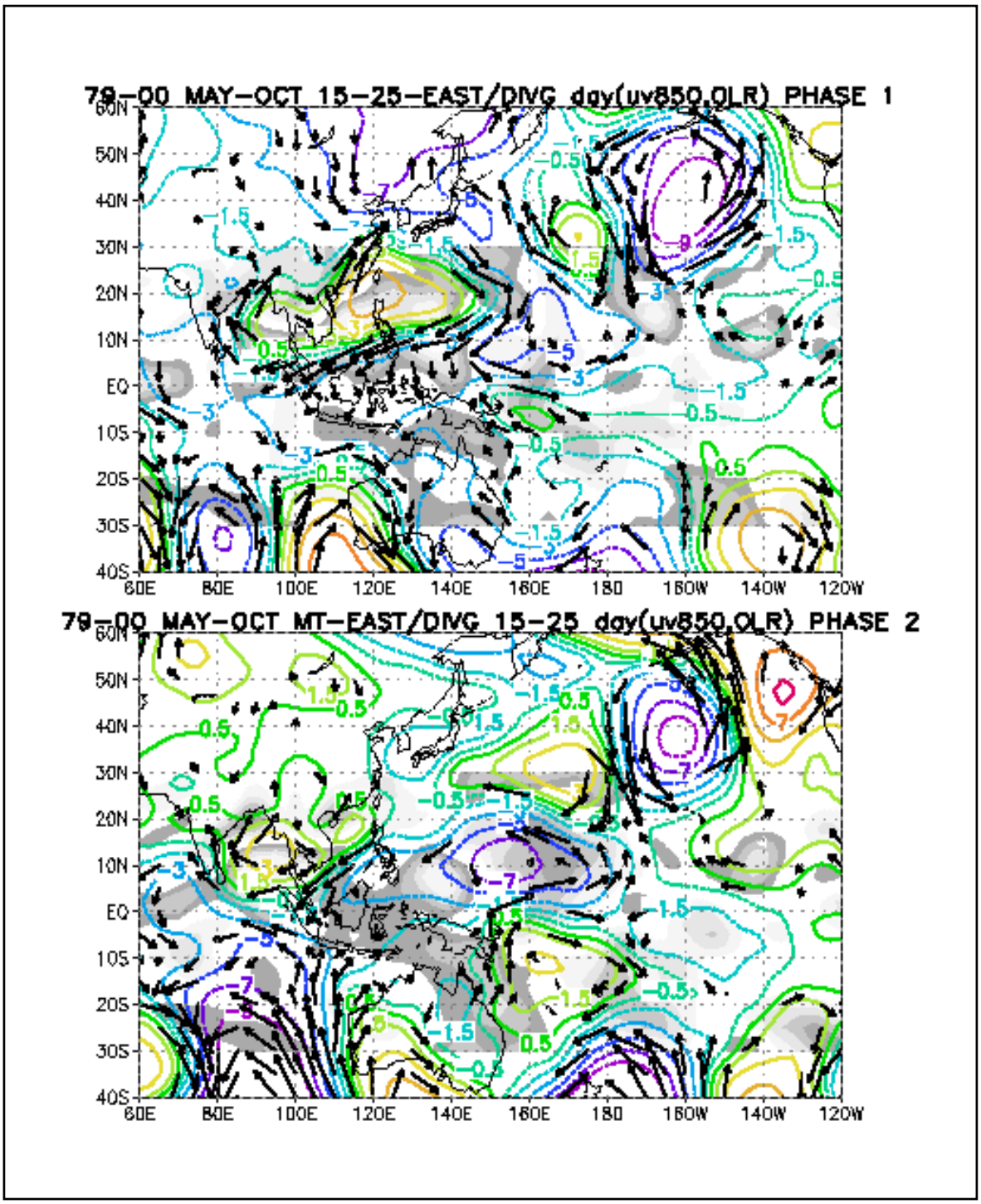

Figure 24. As in Fig. 8, except cases when there was easterly shear and zonal divergence.

D. RELATIONSHIPS WITH TROPICAL CYCLONES

Tropical cyclone occurrences during 1979 to 2000 are depicted by the vertical bars in Figures 4, 5, and 6 with respect to the SVD coefficients. The occurrences that fall within the active periods defined by the SVD modes 1 and 2 will be used for comparison against the composites. The tropical cyclones are grouped by geographical locations in the aforementioned figures:

- N-MT: north of the monsoon trough (20ºN-35ºN, 110ºE-165ºE)
- E-MT: east of the monsoon trough (equator-20ºN,150ºE-180º)
- SCS: South China Sea (equator-20ºN, 100ºE-120ºE)
- MT: monsoon trough (equator-20ºN, 120ºE-150ºE).

To increase the tropical cyclone sample sizes, the occurrences are grouped into only four phases (A-D), which are just the combination of the eight phases (e.g., phases 1 and 2, phases 3 and 4, etc.), and displayed in Table 1. A Chi-squared test for independence between the rows and columns was performed (Anderson and Finn 1996). The null hypothesis is that tropical cyclone occurrences in the four sub-regions are not related to the phase of the SVD-based circulation patterns. The alternate hypothesis is that tropical cyclone occurrence is related to the circulation patters. Since there were nine degrees of freedom (number of columns minus one times number of rows minus one), the critical Chi-squared value was 16.9. Because the observed Chi-square value was calculated to be 22.8, the null hypothesis was rejected at a significance level of 0.01. Thus, the conclusion is that the phase of the SVD-based circulation pattern is related to tropical cyclone occurrence. For comparison, Table 2 shows the expected frequency of tropical cyclone occurrence based on chance. The expected frequencies are computed for each cell i, j as the product of the marginal row total for row i times the marginal column total for column j divided by the total number of tropical cyclones in the table.

TC Region	Phase A	Phase B	Phase C	Phase D	Grand Total
N-MT (-10)	8	7	7	11	33
E-MT (-5)	10	12	8	9	39
SCS (5)	3	11	8	2	24
MT (10)	29	37	15	6	87
Grand Total	50	67	38	28	183

Table 1. Tropical cyclone observations during 1979-2000 that occur during the same time frame as the composites.

TC Region	Phase A	Phase B	Phase C	Phase D
N-MT (-10)	9.02	12.08	6.85	5.049
E-MT (-5)	10.7	14.28	8.1	5.967
SCS (5)	6.56	8.787	4.98	3.672
MT (10)	23.8	31.85	18.1	13.31

Table 2. Tropical cyclone frequencies that would be expected due purely to chance by region and phase.

1. Overall Tropical Cyclone Activity

The overall tropical cyclone activity will first be examined in relation to the circulation patterns that existed for various phases of the active 15- to 25-day cycles. The activity will then be examined in relation to circulation patterns when there is easterly vertical wind shear and either zonal wind convergence or zonal wind divergence.

a. Phase A

Tropical cyclone activity that occurred during 15- to 25-day period for phases 1 and 2 (Fig. 25) is spread uniformly throughout the western North Pacific monsoon trough region, with only a few formations too far north to be

associated to monsoon trough variations on the 15- to 25- day period. Formation primarily occurs along a southeast to northwest axis in the western North Pacific, which corresponds to the general circulation pattern of a large cyclonic anomaly in this location with a similar orientation (Fig. 7).

b. Phase B

During phases 3 and 4 (Fig. 26), tropical cyclone activity begins to shift to a more southwest-northeast oriented axis and occur farther west than in phase A. During this phase, the cyclonic anomaly 2 has moved to the northwest (Fig. 8) and an anticyclonic anomaly (labeled 5 in Fig. 8) is beginning to appear over the equatorial central Pacific.

c. Phase C

During phases 5 and 6 (Fig. 27), tropical cyclone activity is significantly reduced over the eastern Philippine Sea. A southwest to northeast axis of activity is more pronounced than in earlier phases. There is more of a concentration of activity over the South China Sea that occurs near the cyclonic anomaly (circulation 2 in Fig. 9) and extends westward (circulation 2a in Fig. 9). The primary circulation pattern during this phase is a cyclonic anomaly with a southwest-northeast orientation that is moving northwestward and an increasing anticyclonic anomaly 5 in the central North Pacific that is beginning to move northwestward.

d. Phase D

During phases 7 and 8 (Fig. 28), formation occurrences decrease significantly in the western North Pacific and South China Sea since the primary circulation anomaly is anticyclonic. There is an increase in formation occurrence in the central North Pacific, primarily east of 150°E due to the development of a cyclonic anomaly (circulation 4 in Fig. 10) in this region. The reduction in tropical cyclone activity over the South China Sea is dramatic, but this is consistent with the anomalous cyclonic circulation (2a in Fig. 9) having moved westward to the Bay of Bengal. During these phases (7 and 8), tropical cyclone activity is beginning again over the extreme eastern portion of the basin as the next cyclonic anomaly is approaching from the east (circulation 8 in Fig. 10).

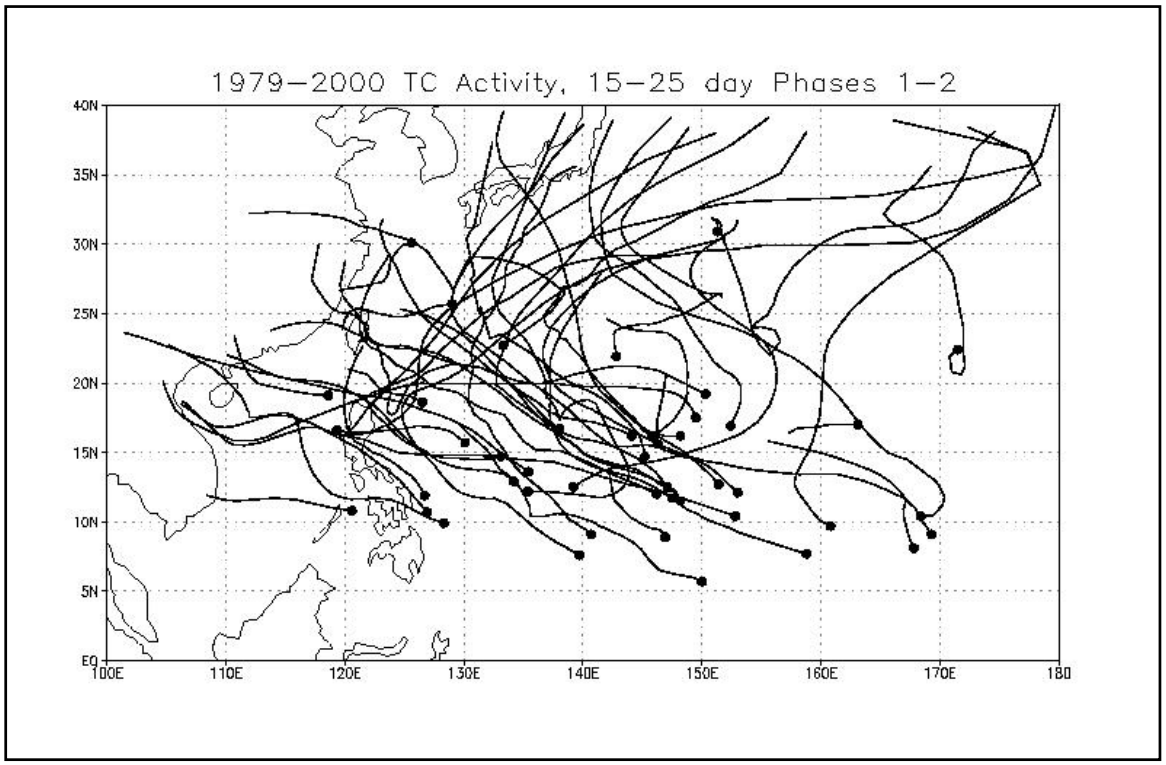

Figure 25. Phase A TC formation (dots) and tracks.

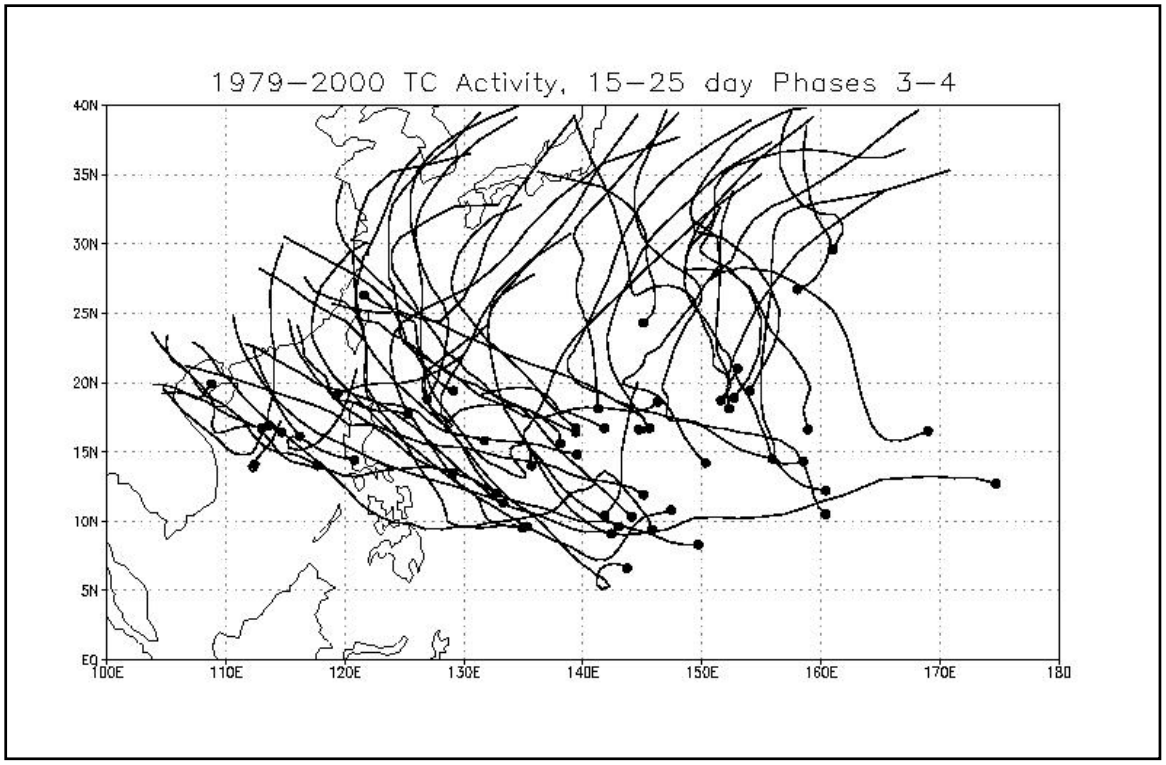

Figure 26. Phase B TC formation (dots) and tracks.

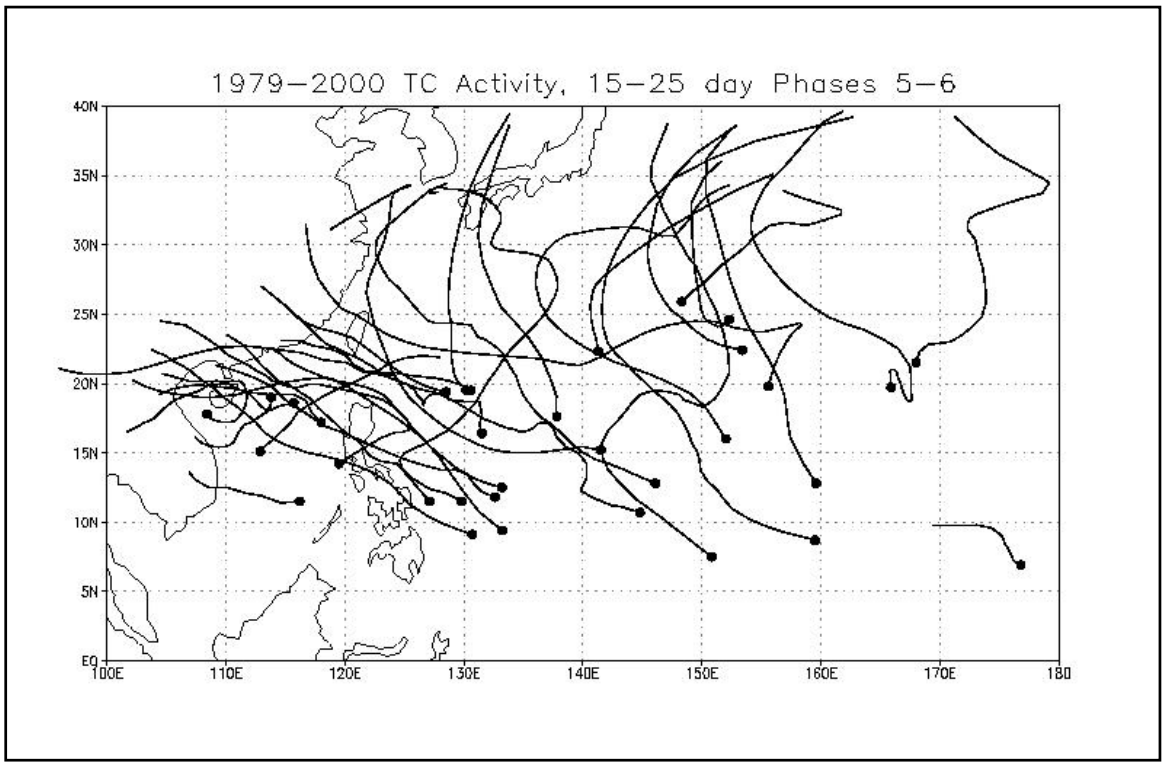

Figure 27. Phase C TC formation (dots) and tracks.

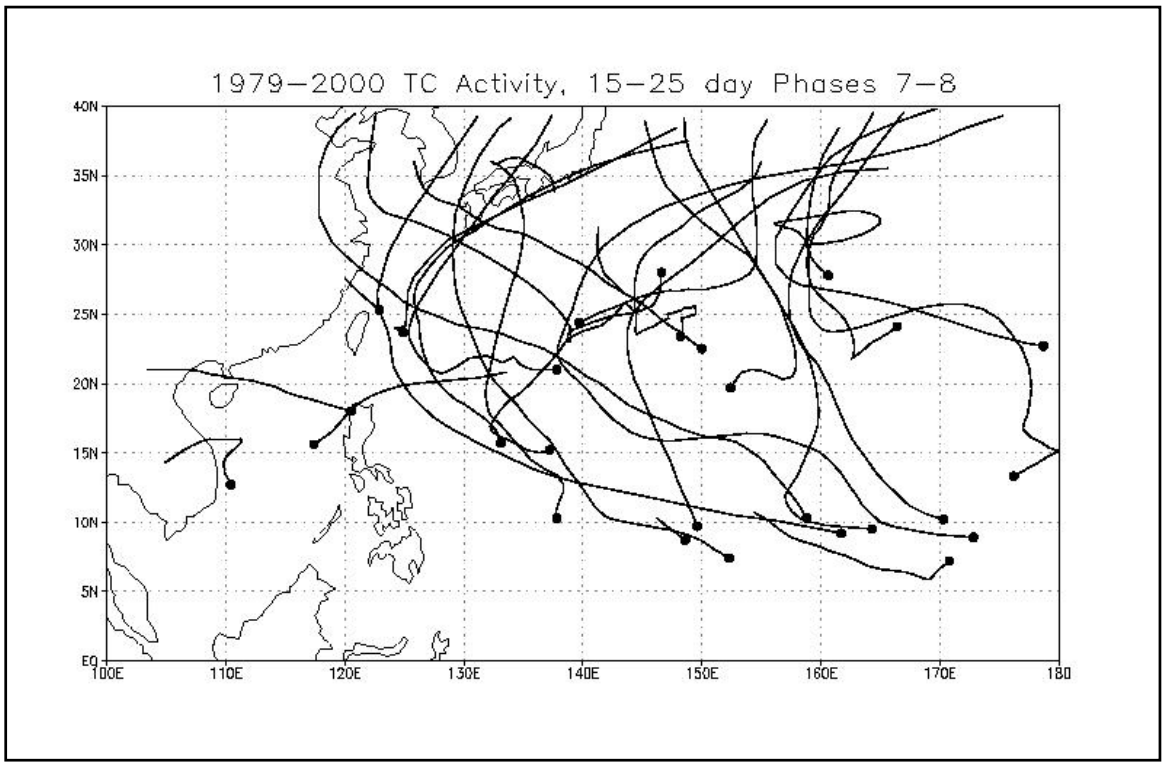

Figure 28. Phase D TC formation (dots) and tracks.

2. Tropical Cyclone Activity: Easterly Vertical Shear with Convergence

a. Phase A

During phases 1 and 2 with an easterly vertical shear environment with zonal wind convergence in the region equator-10ºN, 140ºE-160ºE, (Fig. 29), the majority of tropical cyclones develop over the Philippine Sea, which is expected since the zonal wind convergence is at a maximum near 150°E. Additionally, these tropical cyclones form in the region of the cyclonic anomaly (circulation 2 in Fig. 7) and along the axis of strongest flow between the anticyclonic and cyclonic anomalies.

b. Phase B

During phases 3 and 4 with mean easterly shear and convergence (Fig. 30), tropical cyclones still form primarily in the western North Pacific between 140°E and 150°E. However, they also form farther north than those in phase A as the axis of formation is oriented more southwest to northeast. During these cases, the cyclonic anomaly (2 in Fig. 7) has moved northwestward, and has amplified.

c. Phase C

During phases 5 and 6 (Fig. 31), tropical cyclones form primarily in the South China and western Philippine Seas as the cyclonic anomaly moves farther to the northwest and an anticyclonic anomaly moves into the eastern portion of the basin. The increased activity in the South China Sea is consistent with the extension of the cyclonic anomaly southwestward into the equatorial region of Indochina.

d. Phase D

During phases 7 and 8 (Fig. 32), tropical cyclone formation is absent in the South China Sea and is at a minimum in the far western North Pacific since the region is dominated by an anticyclonic anomaly. Tropical cyclone activity is beginning again over the equatorial central Pacific as the next cyclonic anomaly begins to develop.

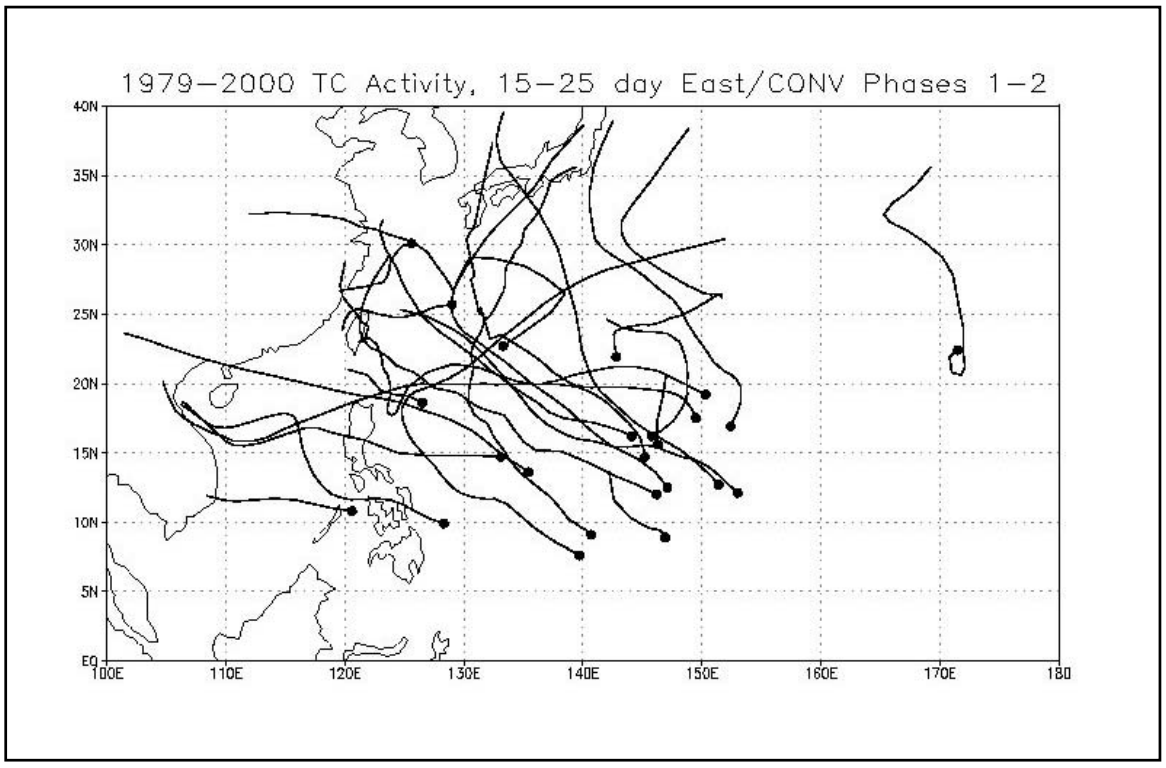

Figure 29. TC formation (dots) and tracks during Phase A when easterly vertical shear exists with convergence conditions.

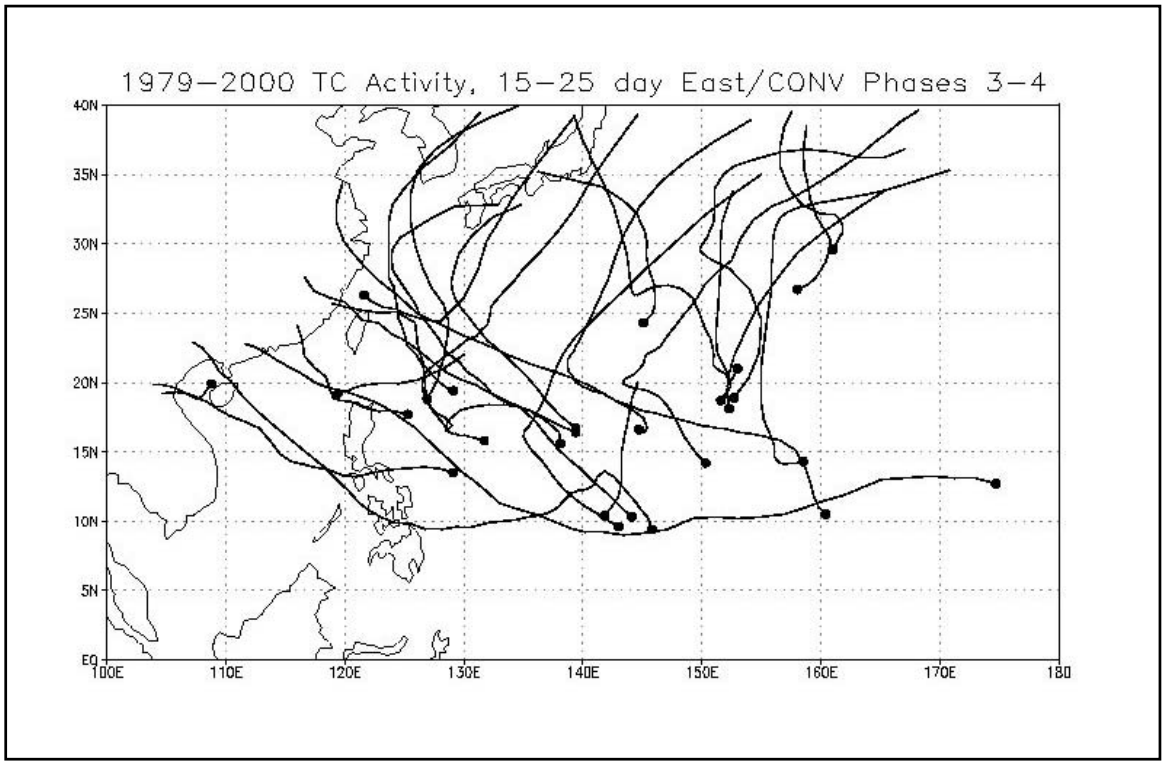

Figure 30. As is in Fig. 29, except during Phase B.

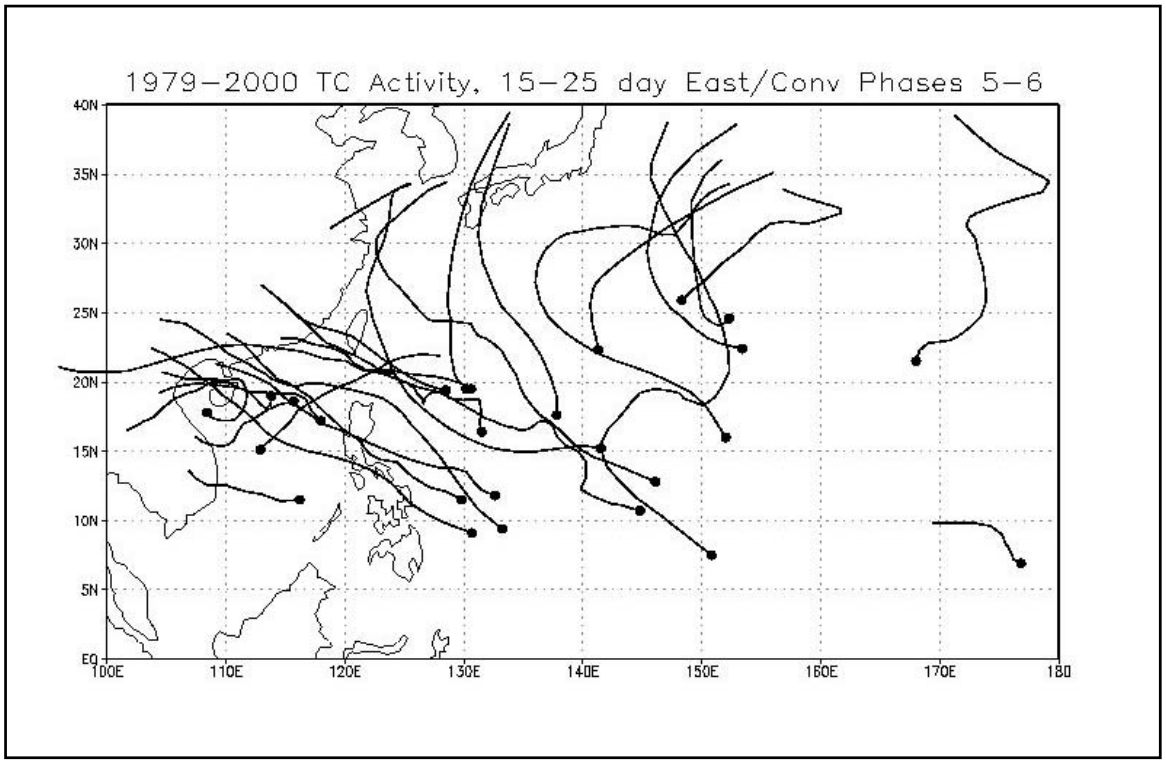

Figure 31. As is in Fig. 29, except during Phase C.

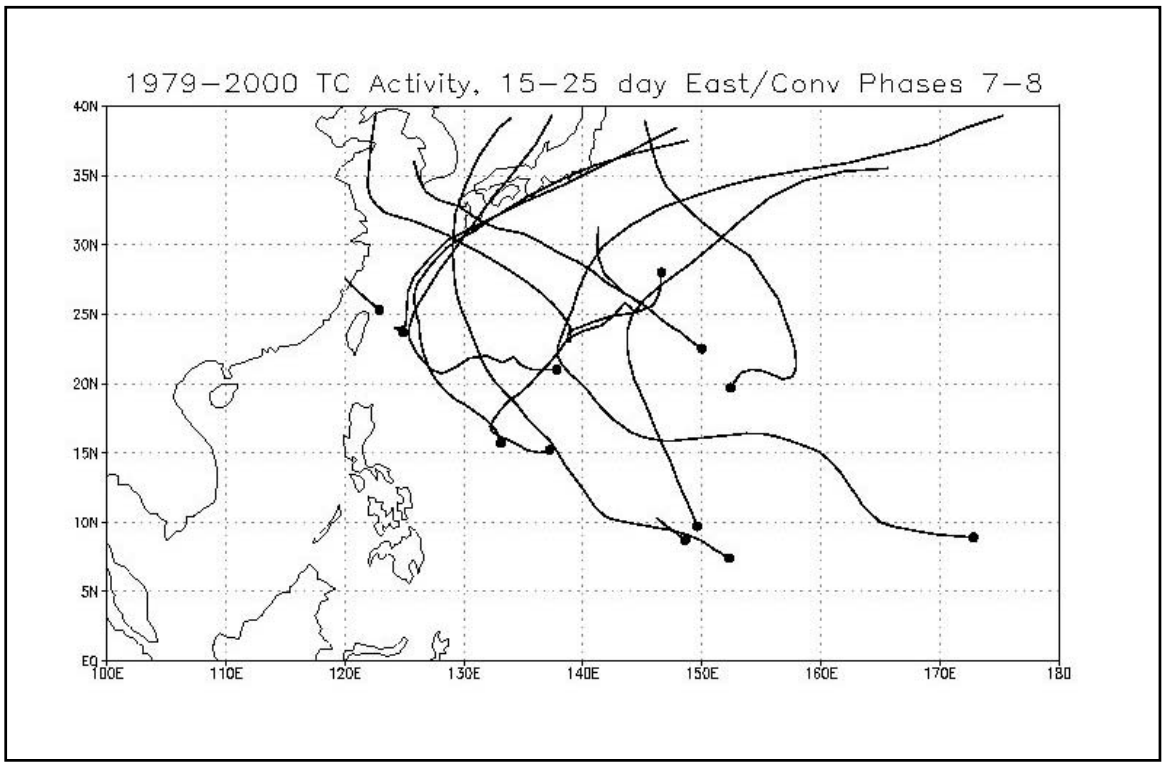

Figure 32. As is in Fig. 29, except during Phase D.

3. Tropical Cyclone Activity: Easterly Vertical Shear with Divergence

It is important to note differences in tropical cyclone activity between phases A and B in the zonal convergence case (Figs. 29, 30) and phases A and B in the zonal divergence case (Figs. 33, 34).

a. Phase A

In the case of zonal divergence, the cyclonic anomaly 2 maintains a more zonal orientation with less northwestward movement over the Philippine Sea. In addition, the cyclonic anomaly intensifies farther east as it interacts with low-level westerly flow that is eastward of the zonal wind convergence case. In Figure 33, the majority of the tropical cyclone activity occurs over the eastern portion of the Philippine Sea and central North Pacific. This corresponds to the area of maximum local westerlies in Figure 22. The formation axis is approximately parallel to the equator. Thus, the circulation characteristics are consistent with the tropical cyclone activity as there are more cases of tropical cyclones in the southeast portion of the basin in the zonal wind divergence cases than in the zonal wind convergence cases.

b. Phase B

In Figure 34, a greater number of tropical cyclones form in the South China and Philippine Seas. However, tropical cyclone activity continues to occur in the central North Pacific but the axis of formation has moved north to along 15°N. As in phase A, the tropical cyclone activity is generally consistent with the circulation characteristics during easterly vertical shear with divergence (Fig. 24).

c. Phase C

In Figure 35, tropical cyclone formation is at a minimum since the western North Pacific is dominated by an anticyclonic anomaly (5 in Fig. 9) in this phase. The few cyclones that do form are near the Philippines and in the central North Pacific near 160°E.

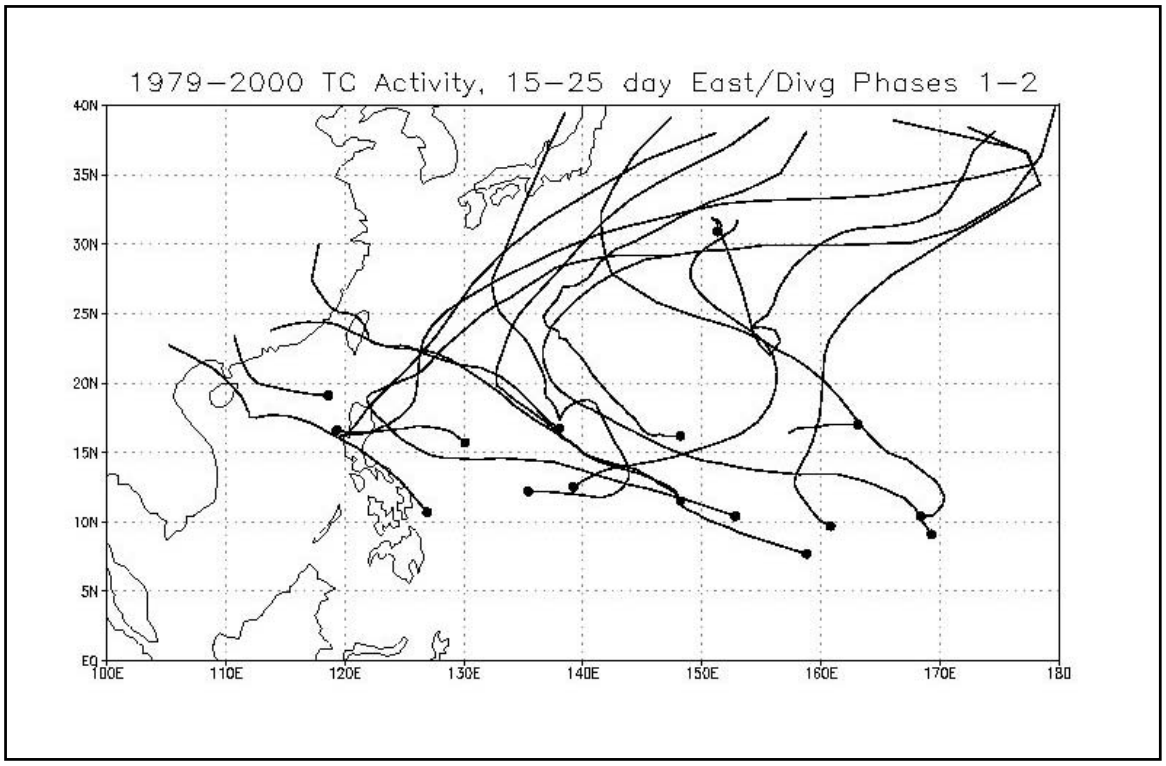

Figure 33. TC formation (dots) and tracks during phase A when easterly vertical shear exists with divergence conditions.

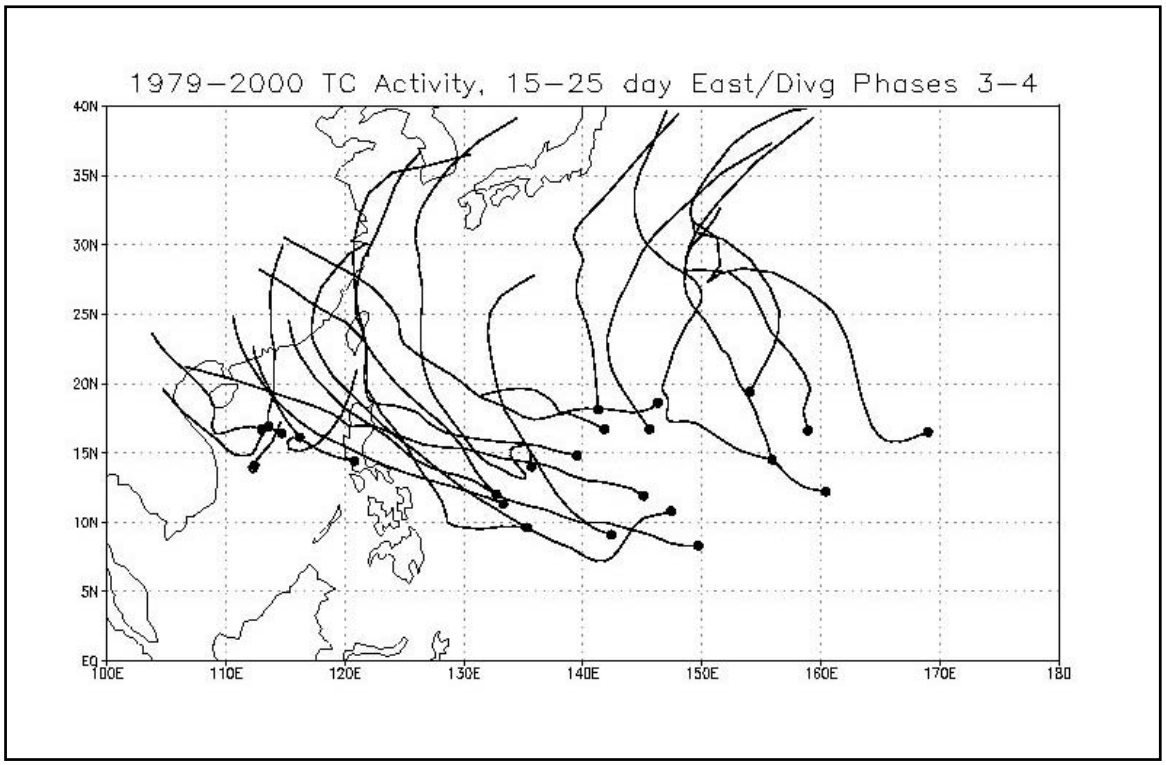

Figure 34. As in Fig. 33 , except during phase B.

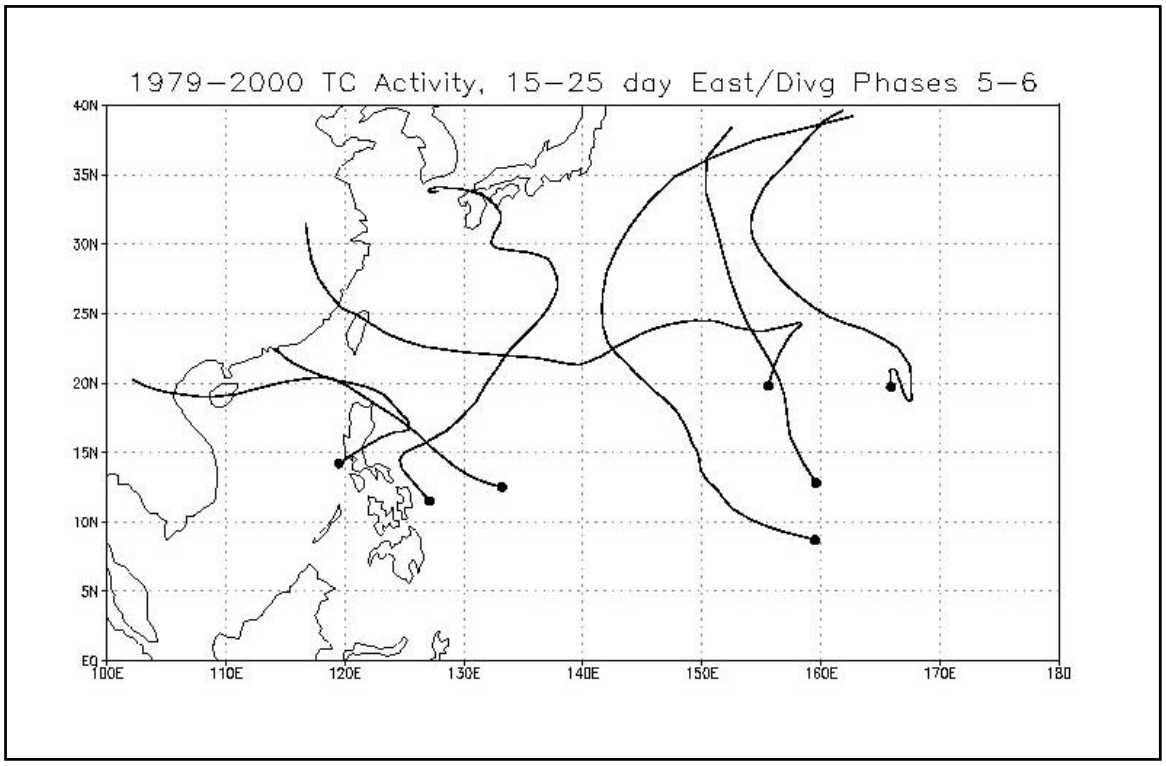

Figure 35. As in Fig. 33, except during phase C.

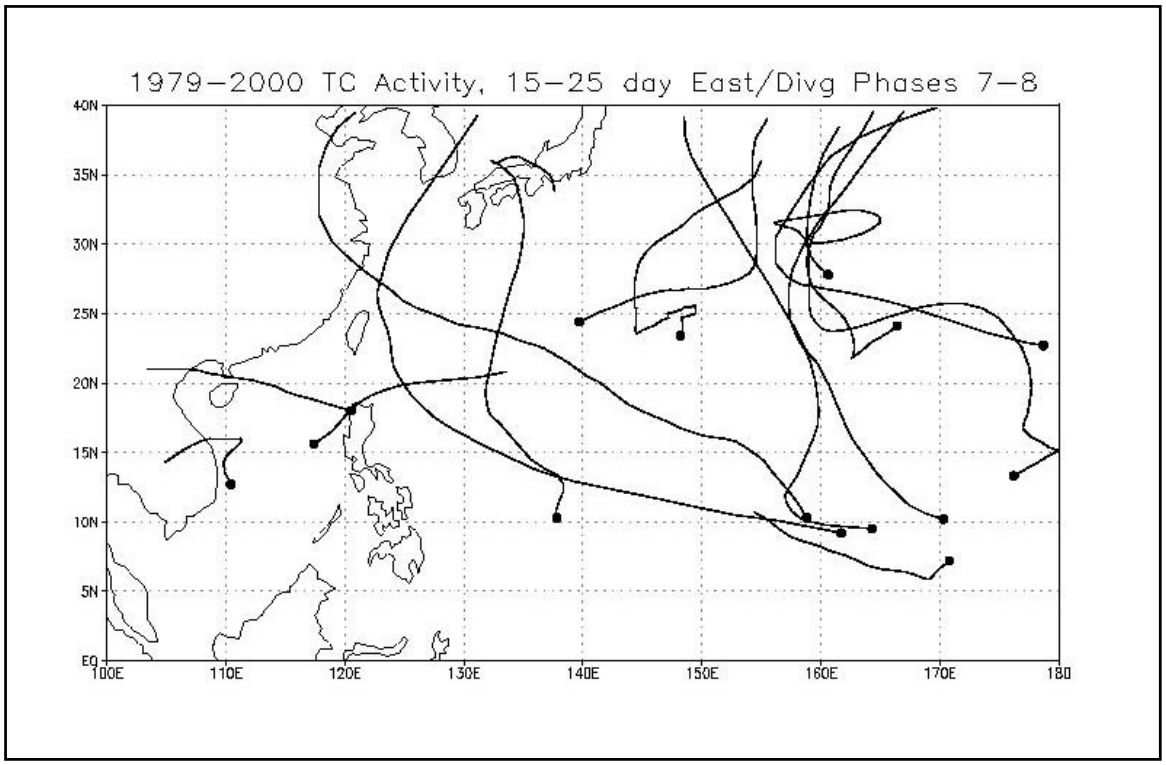

Figure 36. As in Fig. 33, except during phase D.

d. Phase D

In Figure 36, the tropical cyclone activity increases in the central North Pacific east of 160°E in the region of the developing cyclonic anomaly. Activity also increases in the subtropics northeast of the anticyclonic anomaly.

The character of the tropical cyclone activity during the easterly vertical wind shear and zonal divergence is similar to annual shifts in tropical cyclone activity during El Niño years. In fact, 17 of the 50 cases of easterly vertical shear and zonal divergence correspond to an El Niño year (Table 3). Therefore, the significant impact on the altered basic flow over the equatorial western Pacific during El Niño events also impacts the 15-25 day wave pattern in such a way that is consistent with the observed shift in tropical cyclone activity toward the equatorial central Pacific.

Number	Date (yymmdd)	ENSO State
1	800709	NEUTRAL
2	800922	NEUTRAL
3	870922	WARM
4	900613	NEUTRAL
5	920823	NEUTRAL
6	920911	NEUTRAL
7	930924	NEUTRAL
8	940702	WARM
9	940809	WARM
10	940827	WARM
11	940914	WARM
12	970523	WARM
13	970702	WARM
14	970722	WARM
15	970908	WARM
16	970926	WARM
17	971010	WARM

Table 3. Dates of 15-25 day cycles classified as having easterly vertical wind shear and zonal divergence during Phase 1 with respect to the state of the El Nino-Southern Oscillation (ENSO). The ENSO state is defined from the National Centers for Environmental Prediction / Climate Prediction Center classification available at: http://www.cpc.ncep.noaa.gov/products/analysis_monitoring/ensostuff/ensoyears.html.

THIS PAGE INTENTIONALLY LEFT BLANK

IV. CONCLUSION

A. SUMMARY

Singular value decomposition has been used to determine the 15- to 25-day large-scale wave patterns in the western North Pacific during northern summer. Composites constructed from the leading two SVD modes defined the structural characteristics of the wave patterns throughout eight phases.

1. Structural Characteristics

The structural characteristics of the wave patterns were examined in the framework of equatorial Rossby waves forced by tropical heating and their emanation into the mid-latitudes. A key feature is that one of the perturbations downstream in the wave patterns then extends toward the tropics and contributes to the westward-moving equatorial disturbances that have an equatorial Rossby wave structure. These equatorial disturbances have a westward phase speed with an eastward group velocity in both hemispheres. The southern equatorial disturbance appears to be connected with a mid-latitude wave train. This pattern begins over the southern mid-latitudes west of Australia and arcs toward the equator such that its most equatorward penetration east of Australia phases with the westward-moving coupled equatorial circulation. These disturbances appear in both hemispheres as coupled circulations that straddle the equator. However, the Southern Hemisphere disturbance weakens as it propagates westward. The cyclonic anomalies are shown to be associated with equatorial westerlies and enhanced convection, while anticyclonic anomalies are associated with equatorial easterlies and reduced convection.

The overall structural evolution throughout the cycle is summarized by the schematic in Figure 37. The evolution is one of alternating cyclonic and anticyclonic equatorial anomalies. Over the western North Pacific, the northern equatorial anomalies increase in amplitude, shorten in wavelength, refract away from the equator, and become a source for wave propagation into the mid-latitudes (dark gray arrow in Fig. 37). A portion of the northern cyclonic

circulation continues moving westward to the Indian Ocean (light gray arrow in Fig. 37). Downstream disturbances over the mid-latitudes (checked arrow in Fig. 37) contribute to the generation of new equatorial disturbances (diagonally striped arrows in Fig. 37) in a manner similar to that defined by Kiladis and Wheeler (1995) during the northern winter. During periods of zonal wind divergence in the region equator-10ºN, 140ºE-160ºE, new equatorial disturbances appear to originate farther eastward over the eastern North Pacific (dashed arrow in Fig. 37).

Finally, the southern equatorial circulation phases with the Southern Hemisphere mid-latitude wave patterns to accentuate the equatorward penetration of wave energy that contributes to the perturbation growth and areas of anomalous convection over the equatorial western Pacific.

The 15- to 25-day cycle strongly influences tropical cyclone activity (Table 3). The circulation changes during the cycle affect not only the number of cyclones formed, but also the formation location (Figs. 25-28).

2. Variability

Some of the variability in the overall circulation pattern may be attributed to the changes in the basic state, and specifically vertical wind shear and convergence or divergence of the zonal wind. The influence of westerly vertical shear was not examined due to the infrequent occurrence of this environment in the cases used to construct the composites. For those 15- to 25- day cycles in an environment of easterly vertical shear with convergence, westward-moving waves propagate farther into the western Pacific. The wavelength shortens and the cyclonic wave axis orientation changes from zonal to southwest-northeast. The waves also appear to be coupled with the Southern Hemisphere mid-latitude wave train. In an environment of easterly vertical wind shear with zonal wind divergence due to a westerly wind maximum between 160°E and the dateline, wave activity increases farther east than in the zonal wind convergent cases. A strong wave emanation occurs into the Northern Hemisphere mid-latitudes from the central equatorial Pacific. Equatorial circulations maintain a longer

wavelength and a more zonal orientation. In the divergent cases, there does not appear to be a linkage with the Southern Hemisphere mid-latitude wave. In several aspects of the circulation, this basic state may be analogous to a warm ENSO basic state, and 17 of the 50 cases do indeed occur during El Niño years (Table 3).

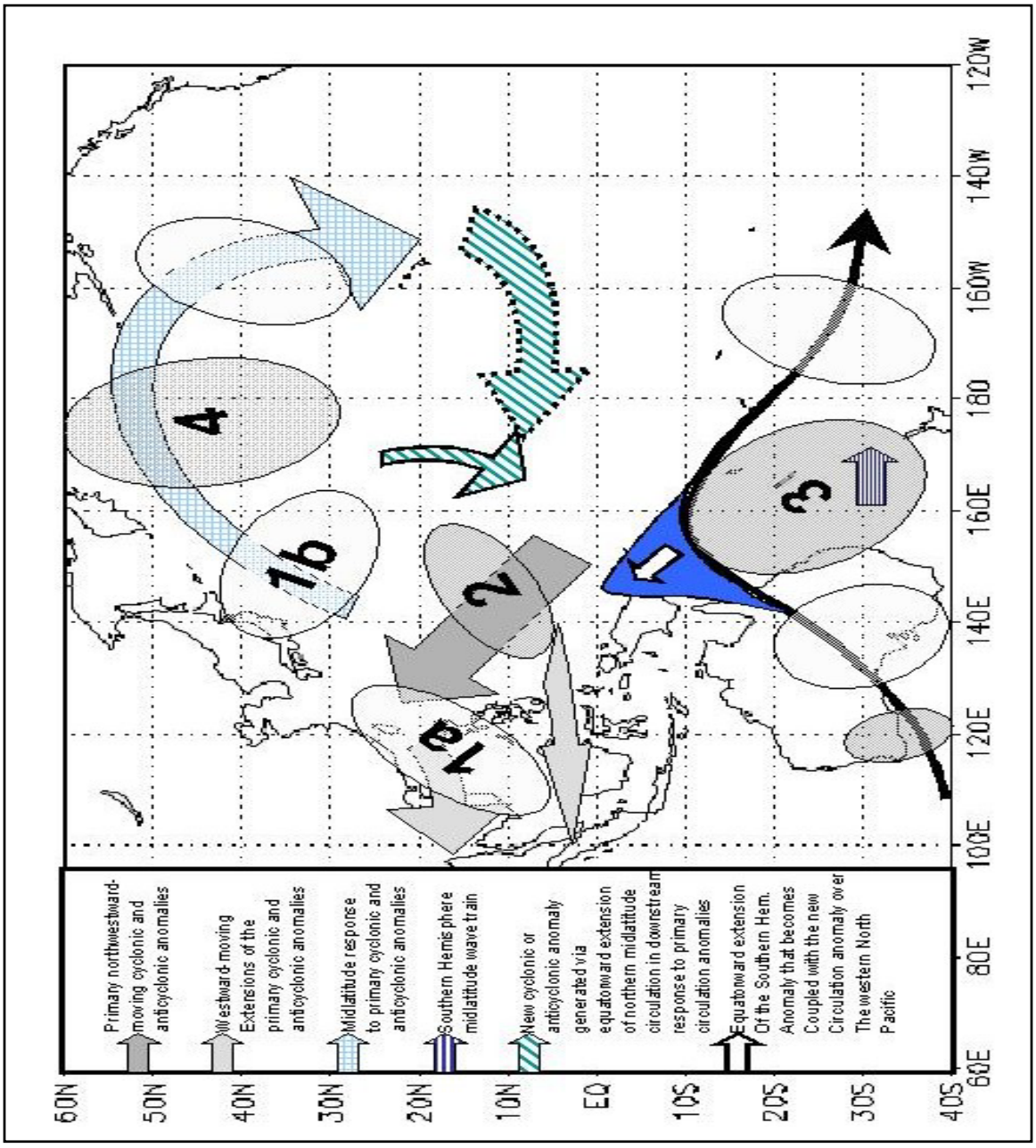

Figure 37. Schematic diagram of 15-25 day wave patterns. Characteristic circulations are numbered as they exist in phase 2 (Fig. 7 (bottom)).

3. Impact on Tropical Cyclone Activity

A statistically significant relationship exists between the 15-25 day wave activity and tropical cyclone occurrence over the western North Pacific. These relationships include the frequency and location of tropical cyclones. An important aspect is the difference in tropical cyclone characteristics between 15-25 day wave activity during times of zonal wind convergence and zonal wind divergence. Tropical cyclones formations tend to be shifted eastward during periods of zonal wind divergence, which is consistent with the eastward shift of the equatorial Rossby-wave activity. In addition, tropical cyclone activity does not progress into the subtropics as much as during the progression of the 15-25 day pattern during periods of zonal convergence. This reduced progression is due to the reduced refraction of the waves in the divergent basic state.

The tropical cyclone activity during periods of zonal divergence is similar to that observed during warm ENSO events. In fact, a majority of the zonal wind divergent cases occurred during warm event years. Therefore, this significant impact of the interannual circulation on the intraseasonal wave activity contributes to a reinforcement of the shift in tropical cyclone activity during warm (and cold) ENSO periods.

B. FUTURE STUDY

This study examined the variability and structure of the wave patterns in the 15- to 25-day period in the Northern Hemisphere summer. Additionally, several aspects of observed tropical cyclone activity, primarily formation areas, are affected by both variations in the basic state and the phase of the wave patterns. Areas for future research should include studies to determine mechanisms within the pattern that contribute to tropical cyclone formation, intensification, and decay as well as track modification.

An important extension would be to analyze these results for predictors of 15-25 day circulation anomalies that could be used as guidance for tropical cyclone formation forecasts on intraseasonal time scales. As a first step, linear

models that utilize the SVD framework should be investigated for perturbations of SVD mode coefficients that would then be used to specify likely circulation patterns.

THIS PAGE INTENTIONALLY LEFT BLANK

LIST OF REFERENCES

Aiyyer, A. R., and J. Molinari, 2003: Evolution of mixed Rossby-gravity waves in idealized MJO environments. *J. Atmos. Sci.,* **60**, 2837-2855.

Anderson, T. W., and J. D. Finn, 1996: *The New Statistical Analysis of Data.* Springer-Verlag, New York, New York, 712 pp.

Arkin, P., and P. J. Webster, 1985: Annual and interannual variability of the tropical-extratropical interaction: An empirical study. *Mon. Wea. Rev.*, **113**, 1510-1523.

Bretherton, C. S., C. Smith, and J. M. Wallace, 1992: An intercomparison of methods for finding coupled patterns in climate data. *J. Climate,* **5**, 541-560.

Chan, J. C. L., 1999: Tropical cyclone activity over the western North Pacific associated with El Niño and La Niña events. *J. Climate*, **13**, 2960-2972.

Clark, V., 2002: Sea power 21: Projecting joint capabilities, *U.S. Naval Institute Proceedings,* **128**, 32-44.

Dickinson, M., and J. Molinari, 2002: Mixed Rossby-gravity waves and western Pacific tropical cyclogenesis. Part I: Synoptic evolution. *J. Atmos. Sci.,* **59**, 2183-2196.

Duchon, C. E., 1979: Lanczos filtering in one and two dimensions. *J. Appl. Meteor.,* **18**, 1016-1022.

Gill, A., 1980: Some simple solutions for heat-induced tropical circulation. *Quart. J. Roy. Meteor. Soc.*, **106**, 447-462.

Gill, A. E., 1982: *Atmosphere-Ocean Dynamics.* Academic Press, 662 pp.

Harr, P. A., and R. L. Elsberry, 1991: Tropical cyclone track characteristics as a function of large-scale circulation anomalies. *Mon. Wea. Rev.,* **119**, 1448-1468.

--, 1995: Large-scale circulation variability over the tropical western North Pacific. Part I: Spatial patterns and tropical cyclone characteristics. *Mon. Wea. Rev.,* **123**, 1225-1246.

Hoskins, B. J., and D. Karoly, 1981: The steady linear response of a spherical atmosphere to thermal and orographic forcing. *J. Atmos. Sci*., **38**, 1179-1196.

Kalnay, E. and Co-Authors, 1996: The NCEP/NCAR 40-year Re-analysis Project. *Bull. Amer. Meteor. Soc.,* **77**, 437-471.

Kiladis, G. N., 1998: Observations of Rossby waves linked to convection over the eastern tropical Pacific. *J. Atmos. Sci.,* **55**, 321-339.

--, and M. Wheeler, 1995: Horizontal and vertical structure of observed tropospheric equatorial Rossby waves. *J. Geophys. Res.,* **100**, 22 981 – 22 997.

Liebmann, B., and H. H. Hendon, 1990: Synoptic-scale disturbances near the equator. *J. Atmos. Sci.,* **47**, 1463-1479.

-- and C. A. Smith, 1996: Description of a complete (interpolated) outgoing long-wave radiation dataset. *Bull. Amer. Meteor. Soc.,* **77**, 1275-1277.

--, H. H. Hendon, and J. D. Glick, 1994: The relationship between tropical cyclones of the western Pacific and Indian oceans and the Madden-Julian oscillation. *J. Meteor. Soc. Japan*, **72**, 401-411.

Lim, H., and C. P. Chang, 1983: Dynamics of teleconnections and Walker circulation forced by equatorial heating. *J. Atmos. Sci.,* **40**, 1897-1915.

Madden, R. A., and P. R. Julian, 1994: Observations of the 40-50 day tropical oscillation – A review. *Mon. Wea. Rev*., **122**, 814-837.

Matsuno, T., 1966: Quasi-geostrophic motions in the equatorial area. *J. Meteor. Soc. Jpn.,* **44**, 25-42.

Rasmussen, E. M., and T. H. Carpenter, 1982: Variations in tropical sea surface temperature and surface wind fields associated with the Southern Oscillation/El Niño. *Mon. Wea. Rev,* **110**, 354-384.

Straub, K. H. and G. N. Kiladis, 2003a: Extratropical forcing of convectively coupled Kelvin waves during austral winter. *J. Atmos. Sci.,* **60**, 526-543.

--, 2003b: The observed structure of convectively coupled Kelvin waves: comparison with simple models of coupled wave instability. *J. Atmos. Sci.,* **60**, 1655-1668.

Takayuba, Y. N., and T. Nitta, 1993: 3-5 day-period disturbances coupled with convection over the tropical Pacific Ocean. *J. Meteor. Soc. Jpn.,* **71**, 221-246.

Wang, B, and X. Xie, 1996: Low-frequency equatorial waves in vertically sheared zonal flow. Part I: Stable waves. *J. Atmos. Sci.,* **53**, 449-467.

Webster, P. J., 1972: Response of the tropical atmosphere to local steady forcing. *Mon. Wea. Rev.,* **100**, 518-541.

--, and H. R. Chang, 1988: Equatorial energy accumulation and emanation regions: Impacts of a zonally varying basic state. *J. Atmos. Sci.,* **45**, 803-829.

Wheeler, M., and G. Kiladis, 1999: Convectively coupled equatorial waves: Analysis of clouds and temperature in the wavenumber-frequency domain. *J. Atmos. Sci*., **56**, 374-399.

THIS PAGE INTENTIONALLY LEFT BLANK

INITIAL DISTRIBUTION LIST

1. Defense Technical Information Center
   Ft. Belvoir, VA

2. Dudley Knox Library
   Naval Postgraduate School
   Monterey, CA

3. Dr. M. Steven Tracton
   Office of Naval Research
   Arlington, VA

4. Professor Carlyle Wash
   Naval Postgraduate School
   Monterey, CA

5. Professor Philip Durkee
   Naval Postgraduate School
   Monterey, CA

6. Professor Russell Elsberry
   Naval Postgraduate School
   Monterey, CA

7. Professor Patrick Harr
   Naval Postgraduate School
   Monterey, CA

8. Director, Joint Typhoon Warning Center
   Naval Pacific Meteorology and Oceanography Center
   Pearl Harbor, HI

9. Lieutenant Tracey Delk
   United States Naval Academy
   Annapolis, MD